Available online at www.sciencedirect.com

ScienceDirect

Journal of Differential Equations 357 (2023) 32–63

Journal of Differential Equations

www.elsevier.com/locate/jde

Bifurcation analysis in a diffusive predator-prey model with spatial memory of prey, Allee effect and maturation delay of predator

Shuai Li [a], Sanling Yuan [a,*], Zhen Jin [b], Hao Wang [c]

[a] *College of Science, University of Shanghai for Science and Technology, Shanghai 200093, China*
[b] *Complex Systems Research Center, Shanxi University, Taiyuan, Shanxi 030006, China*
[c] *Department of Mathematical and Statistical Sciences, University of Alberta, Edmonton, Alberta T6G 2G1, Canada*

Received 17 September 2022; revised 19 January 2023; accepted 2 February 2023

Abstract

In this paper, we formulate a spatial model with memory delay of the prey, Allee effect and maturation delay with delay-dependent coefficients of predators. We first explore the model without delays and diffusions, and find that it can undergo a saddle-node bifurcation when the intensity of Allee effect is at the tipping point. Then for the scenario of stability of the coexistence steady state without delays, we obtain the crossing curves on the delays plane. The model can undergo Hopf bifurcation when delays pass through these crossing curves from a stable region to an unstable one. We further calculate the normal form of Hopf bifurcation and hence obtain the direction of Hopf bifurcation and the stability of the bifurcation periodic solutions. It is shown that the model can possess multiple stability switches and a stable spatially heterogeneous periodic solution with mode-4 as delays vary.

Keywords: Spatial memory; Delay-dependent coefficients; Stability switches; Predator-prey; Normal form

* Corresponding author.
E-mail address: sanling@usst.edu.cn (S. Yuan).

https://doi.org/10.1016/j.jde.2023.02.009
0022-0396/

1. Introduction

Modeling the interplay between the prey and predators has been an active topic in mathematical biology since the seminal work of Lotka-Volterra (LV) [1,2]. Recently, a lot of models have been developed from LV model to elucidate the intricate biological processes more realistically. One pivotal evolvement of LV model is the incorporation of Allee effect which describes the density-mediated decline in intrinsic growth rate at its low densities [3,4]. The Allee effect can take place owing to a great variety of mechanisms as diverse as reproductive facilitation, cooperative hunting and group defense enhancement [5,6]. There are two categories of Allee effect: strong Allee effect and weak Allee effect which can be respectively applied to scenarios where for low population density the growth rate of the population is negative and still positive. Most previous works paid attention to the Allee effect on the prey population and found that Allee effect can alter the dynamics of predator-prey model, especially can induce population collapses to extinction [7–10]. In fact, predators can also exhibit an Allee effect due to reproductive facilitation mechanisms such as sperm limitation, cooperative breeding, difficulty in finding mates, and so on. In this case, the efficiency of the prey conversion largely reduces at low density but increases as the density of predators increases [11–13]. Obviously, these non-hunting mechanisms can be phenomenologically captured by altering the predators' numerical response rather than functional response and are also worth studying.

Another momentous extension of LV model is the incorporation of maturation period of predators since predators require time to mature to multiply their descendants. This biological process can be captured by a model with delay-dependent parameters whose derivation is deduced by solving an age-structured model through the characteristic lines method [14–16]. Time delay can have either a stable or unstable effect on the stability of the developed model due to the occurrence of Hopf bifurcations, relying on the length of the maturation period. This is a striking difference from the classical LV model [17,18]. Taking spatial heterogeneity into account, Xu and Wei recently considered a diffusive budworm model with delay-dependent coefficients and obtained the criteria for the appearance of Hopf bifurcation [19]. The authors in [20] established the algorithm to calculate the normal form near a double Hopf bifurcation and then applied this algorithm to an epidemic model with maturation delay. It is acknowledged that the Hopf bifurcation induced by delay can lead to periodic oscillations and also be one of the precursors to irregular spatiotemporal patterns in spatial models [21,22]. However, the results of models with maturation delay and Allee effect in predators seem rare.

Notice that, the models discoursed thus far do not consider the effects of spatial memory and cognition of animals on their movements. Studying the mechanism of animal movement provides a sound foundation for the exploration of ecological processes [23–25]. Some animals can memorize the historic distribution of their predators. They can thus adopt memory-driven movement to keep away from areas where predators once resided to reduce the ability of predators' acquisition [26–29]. For example, females of woodland caribou (prey) choose previously visited zones to calve since black bears (predator) hunt for ungulate juvenile prey inactively in these zones [30]. Another example is that elks tend to previously visited areas to avoid predation since the spatial distribution of wolves has been stored in their memory [31]. To describe the memory-driven movement, Shi et al. originally put forward a mathematical model by modifying Fick's law by adding an extra directed movement toward the positive or negative gradient of the past fixed time density distribution [32]. Afterward, Song et al. generalized the above model to a class of predator-prey model with memory delay in the predator population [33]. They further overcame the difficulty induced by memory-dependent diffusion to establish an algorithm for

the calculation of Hopf bifurcation normal form [34] and thus found that memory delay can induce a stable spatially heterogeneous periodic solution with mode-2 via destabilizing the steady state. However, the above memory-driven diffusion models do not consider the maturation delay and Allee effect in the predator population. In this paper, we fill up this gap. The highlights and contributions of this paper are as follows.

- A diffusive predator-prey model with memory-driven diffusion and delay-dependent parameters is proposed. The model incorporates many mechanisms as diverse as reproductive facilitation, maturation period, random and directed movement.
- The stability crossing curve method set forth in [35] is creatively applied to the model to study its possible Hopf bifurcations induced by delays.
- Explicit formulas for the coefficients of normal form for the Hopf bifurcation induced by memory delay are obtained by fixing the maturation delay in its stable interval. The question posited in [36] on how to calculate the normal form of the memory-based diffusion model with two different delays is properly solved.
- The model can exhibit stability switches and stable spatially heterogeneous periodic solutions with mode-4, which seem new to previous investigations [32,34,37].

In a nutshell, the methods and results in this paper may provide a theoretical avenue to understand the spatial distribution of species. The remainder of this paper is organized as follows. In Sect. 2, we present our model. In Sect. 3, we derive the conditions on the linear stability and the occurrence of Hopf bifurcation of the model by analyzing its associated characteristic equations. In Sect. 4, we determine the properties of Hopf bifurcation by calculating its normal form. Finally, in Sect. 5, we conclude our paper with some discussions.

2. Model formulation

We formulate our model by incorporating Allee effect, maturation delay as well as spatial memory into the classic LV model. Inspired by the model proposed by Sen et al. in [11], we present the following predator-prey model to mimic the Allee effect in predators:

$$\begin{cases} \frac{\mathrm{d}N}{\mathrm{d}t} = rN\left(1-\frac{N}{K}\right) - bNP, \\ \frac{\mathrm{d}P}{\mathrm{d}t} = \beta NP\frac{P}{h+P} - \mu P, \end{cases} \tag{1}$$

where N and P represent respectively the densities of prey and predator populations; r is the maximum per capita growth rate; K is the carrying capacity; b is the attack rate of predators; β is the total effect to predators by consuming prey; μ stands for the death rate of predators; $\frac{P}{h+P}$ describes the Allee effect in predators with the intensity of Allee effect h [12]. Model (1) can be applied to describe many scenarios, such as describing the mate-finding Allee effect of flour beetles, pelagic fish, whales, and so on; characterizing the low fertilization efficiency of flour beetles, snails and queen conchs at their low densities, and mimicking the cooperative breeding scenario of bird species [11].

Note the fact that predators require time to mature to multiply their descendants. We introduce maturation delay σ to model (1) by dint of the method set forth in [14,15,38] and obtain the following predator-prey model with delay-dependent parameters:

$$\begin{cases} \frac{\mathrm{d}N}{\mathrm{d}t} = rN\left(1-\frac{N}{K}\right) - bNP, \\ \frac{\mathrm{d}P}{\mathrm{d}t} = \beta N_\sigma P_\sigma \frac{P_\sigma}{h+P_\sigma}\mathrm{e}^{-d\sigma} - \mu P. \end{cases}$$

Here P and d represent respectively the density of adult predators and the death rate of juvenile predators; N_σ and P_σ refer to $N(t-\sigma)$ and $P(t-\sigma)$, respectively.

As mentioned in the previous section, prey (such as woodland caribou and elk) can possess spatial memory for predators and thus move away from them according to the accumulation of information in space. We describe this memory-driven movement of prey by modifying Fick's law as established in [32]. Also, we assume that the diffusive ability of immature predators is much smaller than that of mature predators, thus the movement of immature predators during the maturation period is ignorable [39]. The domain species inhabit is closed and one dimension with length $\iota\pi$. We then formulate the following spatial predator-prey model with Neumann boundary conditions:

$$\begin{cases} \frac{\partial N}{\partial t} = \delta_{11}N_{xx} + \delta_{12}\left(NP_x(x,t-\tau)\right)_x + rN\left(1-\frac{N}{K}\right) - bNP, \ 0<x<\iota\pi, \ t>0, \\ \frac{\partial P}{\partial t} = \delta_{22}P_{xx} + \frac{\beta N_\sigma P_\sigma^2}{h+P_\sigma}\mathrm{e}^{-d\sigma} - \mu P, \ 0<x<\iota\pi, \ t>0, \\ N_x(x,t) = P_x(x,t) = 0, \ x = 0, \iota\pi, \ t \geq 0, \end{cases} \tag{2}$$

where $N = N(x,t)$ and $P = P(x,t)$ represent respectively the densities of prey and adult predators at location x and time t; δ_{11} and δ_{12} refer respectively to the random diffusion and memory-dependent diffusion coefficients of the prey; δ_{22} describes random diffusion of predators; τ is the averaged memory period of the prey.

In this paper, we will devote ourselves to the investigation of the impacts of Allee effect, mature delay and memory delay on the spatiotemporal distributions of model (2).

3. Stability and Hopf bifurcation of model (2)

We will study the linear stability and the occurrence of Hopf bifurcation for model (2) with or without diffusions and delays in this section. Biologically, we are interested in the coexistence of the two populations. We first consider the existence of the coexisting constant steady states and then, at which, obtain the corresponding characteristic equations of the associated linear system of model (2).

Notice that if $\bar{E} = (\bar{N}, \bar{P})$ is a positive constant steady state of model (2), it must satisfy $\bar{N} = \dfrac{\mu(h+\bar{P})\mathrm{e}^{d\sigma}}{\beta\bar{P}}$ and $\bar{P}$ is a positive root of the following equation:

$$\beta bK P^2 + (r\mu\mathrm{e}^{d\sigma} - rK\beta)P + r\mu h\mathrm{e}^{d\sigma} = 0. \tag{3}$$

Obviously, Eq. (3) admits two different positive roots if and only if

$$\mu < \beta K\mathrm{e}^{-d\sigma}, \ \ h < h_{SN}(\sigma) := \frac{1}{4}\frac{r(K\beta - \mu\mathrm{e}^{d\sigma})^2\mathrm{e}^{-d\sigma}}{bK\beta\mu}. \tag{4}$$

In this case, model (2) has two positive constant steady states, denoted respectively by $E_1(\sigma) = (N_1(\sigma), P_1(\sigma))$ and $E_2(\sigma) = (N_2(\sigma), P_2(\sigma))$ with $P_1(\sigma) < P_2(\sigma)$. Linearizing model (2) at $E_i(\sigma)$ yields

$$\begin{cases} \frac{\partial N(x,t)}{\partial t} = \delta_{11} N_{xx}(x,t) + \delta_{12} N_i(\sigma) P_{xx}(x,t-\tau) + \alpha_{11}(\sigma) N(x,t) + \alpha_{12}(\sigma) P(x,t), \\ \quad x \in (0, \iota\pi),\ t > 0, \\ \frac{\partial P(x,t)}{\partial t} = \delta_{22} P_{xx}(x,t) + \alpha_{22} P(x,t) + \beta_{21}(\sigma) N(x,t-\sigma) + \beta_{22}(\sigma) P(x,t-\sigma), \\ \quad x \in (0, \iota\pi),\ t > 0, \\ N_x(x,t) = P_x(x,t) = 0, \quad x = 0, \iota\pi,\ t \geq 0, \end{cases} \tag{5}$$

where

$$\alpha_{11}(\sigma) = -\frac{r N_i(\sigma)}{K}, \qquad \alpha_{12}(\sigma) = -b N_i(\sigma), \qquad \alpha_{22} = -\mu,$$

$$\beta_{21}(\sigma) = \frac{\beta P_i^2(\sigma)}{h + P_i(\sigma)} \mathrm{e}^{-d\sigma}, \qquad \beta_{22}(\sigma) = \frac{\beta N_i(\sigma) P_i^2(\sigma) + 2\beta h N_i(\sigma) P_i(\sigma)}{(h + P_i(\sigma))^2} \mathrm{e}^{-d\sigma}.$$

Suppose the eigenfunction of system (5) associated with eigenvalue λ is

$$(N(t), P(t)) = (c_1, c_2) \mathrm{e}^{\lambda t} \cos\left(\left(\frac{n}{\iota}\right) x\right), \tag{6}$$

where $n \in \mathbf{N}_0$ is the wave number. By substituting (6) into system (5), we get

$$\begin{cases} \left(\lambda c_1 + \delta_{11} \left(\frac{n}{\iota}\right)^2 c_1\right) \mathrm{e}^{\lambda t} = (\alpha_{11}(\sigma) c_1 + \alpha_{12}(\sigma) c_2)\, \mathrm{e}^{\lambda t} - \delta_{12} N_i(\sigma) \left(\frac{n}{\iota}\right)^2 c_2 \mathrm{e}^{\lambda(t-\tau)}, \\ \left(\lambda c_2 + \delta_{22} \left(\frac{n}{\iota}\right)^2 c_2\right) \mathrm{e}^{\lambda t} = \alpha_{22} c_2 \mathrm{e}^{\lambda t} + (\beta_{21}(\sigma) c_1 + \beta_{22}(\sigma) c_2) \mathrm{e}^{\lambda(t-\sigma)}, \end{cases}$$

which has a nontrivial solution $(c_1,\ c_2)$ if and only if $\det(\lambda E_2 - J(n;\sigma,\tau)) = 0$, where

$$J(n;\sigma,\tau) = \begin{pmatrix} \alpha_{11}(\sigma) - \delta_{11} \left(\frac{n}{\iota}\right)^2 & \alpha_{12}(\sigma) - \delta_{12} N_i(\sigma) \left(\frac{n}{\iota}\right)^2 \mathrm{e}^{-\lambda\tau} \\ \beta_{21}(\sigma) \mathrm{e}^{-\lambda\sigma} & \alpha_{22} + \beta_{22}(\sigma) \mathrm{e}^{-\lambda\sigma} - \delta_{22} \left(\frac{n}{\iota}\right)^2 \end{pmatrix}. \tag{7}$$

Then we obtain the following characteristic equation:

$$\mathfrak{g}_0^n(\lambda,\sigma) + \mathfrak{g}_1^n(\lambda,\sigma) \mathrm{e}^{-\lambda\sigma} + \mathfrak{g}_2^n(\sigma) \mathrm{e}^{-\lambda(\tau+\sigma)} = 0, \tag{8}$$

where

$$\begin{cases} \mathfrak{g}_0^n(\lambda,\sigma) = \lambda^2 + \mathfrak{g}_{01}^n(\sigma)\lambda + \mathfrak{g}_{00}^n(\sigma), \\ \mathfrak{g}_1^n(\lambda,\sigma) = \mathfrak{g}_{11}^n(\sigma)\lambda + \mathfrak{g}_{10}^n(\sigma), \\ \mathfrak{g}_2^n(\sigma) = \mathfrak{g}_{20}^n(\sigma) \end{cases}$$

with

$$\begin{cases} \mathfrak{g}_{01}^n(\sigma) = \delta_{11}\left(\frac{n}{\iota}\right)^2 + \delta_{22}\left(\frac{n}{\iota}\right)^2 - \alpha_{11}(\sigma) - \alpha_{22}, \\ \mathfrak{g}_{00}^n(\sigma) = \delta_{11}\delta_{22}\left(\frac{n}{\iota}\right)^4 - \delta_{11}\alpha_{22}\left(\frac{n}{\iota}\right)^2 - \delta_{22}\alpha_{11}(\sigma)\left(\frac{n}{\iota}\right)^2 + \alpha_{11}(\sigma)\alpha_{22}, \\ \mathfrak{g}_{11}^n(\sigma) = -\beta_{22}(\sigma), \\ \mathfrak{g}_{10}^n(\sigma) = -\delta_{11}\beta_{22}(\sigma)\left(\frac{n}{\iota}\right)^2 + \alpha_{11}(\sigma)\beta_{22}(\sigma) - \alpha_{12}(\sigma)\beta_{21}(\sigma), \\ \mathfrak{g}_{20}^n(\sigma) = \delta_{12}N_i(\sigma)\left(\frac{n}{\iota}\right)^2\beta_{21}(\sigma). \end{cases}$$

3.1. Stability analysis of model (2) without delays

We first study the long-time behavior of model (2) with no delays and diffusions, i.e., $n = 0$ and $\sigma = \tau = 0$. In this case, (7) becomes

$$J(0;0,0) = \begin{pmatrix} \alpha_{11}(0) & \alpha_{12}(0) \\ \beta_{21}(0) & \alpha_{22} + \beta_{22}(0) \end{pmatrix} = \begin{pmatrix} \frac{-rN_i(0)}{K} & -bN_i(0) \\ \frac{\mu P_i(0)}{N_i(0)} & \frac{\beta h N_i(0) P_i(0)}{(h+P_i(0))^2} \end{pmatrix}.$$

Direct calculations yield

$$\begin{aligned} \det(J(0;0,0)) &= \frac{N_i(0)}{h+P_i(0)}\left(\frac{-r\beta N_i(0)P_i(0)h}{(h+P_i(0))K} + b\beta P_i^2(0)\right) \\ &= \frac{N_i(0)}{h+P_i(0)}\left(\frac{-r\mu h}{K} + b\beta P_i^2(0)\right) \\ &= \frac{r\beta N_i(0)P_i^2(0)}{K(h+P_i(0))}\left(-\frac{\mu h}{\beta P_i^2(0)} - \left(-\frac{bK}{r}\right)\right) \\ &= \frac{r\beta N_i(0)P_i^2(0)}{K(h+P_i(0))}\left(k_2(E_i(0)) - k_1(E_i(0))\right), \end{aligned}$$

where $k_1(E_i(0))$ and $k_2(E_i(0))$ are respectively the derivatives of N-nullcline and P-nullcline at $E_i(0)$. Clearly, at $E_1(0)$, $\det(J(0;0,0)) < 0$ and at $E_2(0)$, $\det(J(0;0,0)) > 0$. Hence $E_1(0)$ is a saddle, and $E_2(0)$ is locally asymptotically stable provided that at $E_2(0)$, $\mathrm{tr}(J(0;0,0)) = \frac{N_2(0)}{K(h+P_2(0))^2}\left(-rP_2^2(0) + h(\beta K - 2r)P_2(0) - rh^2\right) < 0$. We thus have the following results.

Theorem 1. *Model (1) has two positive equilibria $E_1(0)$ and $E_2(0)$ provided that $\mu < \beta K$ and $h < h_{SN}(0)$. Moreover, $E_1(0)$ is a saddle and $E_2(0)$ is locally asymptotically stable if* $\mathrm{tr}(J(0;0,0)) < 0$.

It is easy to see that when $r > \frac{\beta K}{2}$, $\mathrm{tr}(J(0;0,0)) < 0$ at $E_2(0)$. We make the following hypothesis:

(**H**1) $h < h_{SN}(0)$, $\mu < \beta K$ and $r > \frac{\beta K}{2}$.

Remark 1. Model (1) undergoes a saddle-node bifurcation at $h = h_{SN}(0)$. In fact, denote by $U = \left(1, -\frac{r}{bK}\right)^{\mathrm{T}}$ and $W = \left(\frac{\mu K P}{rN^2}, 1\right)^{\mathrm{T}}$ respectively the eigenvectors associated with $\lambda = 0$ of $J(0;0,0)$ and $\lambda = 0$ of $J(0;0,0)^{\mathrm{T}}$, and denote by $F(N,P;h)$ the vector field of model (1).

We can check that $W \cdot F_h(N, P; h) = \frac{-\beta N P^2}{(h+P)^2}\big|_{h=h_{SN}(0)} \neq 0$ and $W \cdot [D^2 F(N, P; h)(U, U)] = \frac{-r^4(K\beta+\mu)(K\beta-\mu)^3}{8\mu K^4\beta^2 b^4 P(h+P)^2}\big|_{h=h_{SN}(0)} < 0$. The assertion follows from the Sotomayor's Theorem [40]. This indicates that once the intensity of the Allee effect exceeds the tipping point $h_{SN}(0)$, predators will go to extinction.

We now deduce the stability conditions of $E_2(0)$ for spatial model (2) in the absence of delays, i.e., $\sigma = \tau = 0$. In this case, at $E_2(0)$, Eq. (8) becomes

$$\lambda^2 - \mathrm{tr}(J(n; 0, 0))\lambda + \det(J(n; 0, 0)) = 0,$$

where

$$\begin{aligned}
\mathrm{tr}(J(n; 0, 0)) &= -(\delta_{11} + \delta_{22})\left(\frac{n}{\iota}\right)^2 + \mathrm{tr}(J(0; 0, 0)),\\
\det(J(n; 0, 0)) &= \left(\delta_{11}\delta_{22}\left(\frac{n}{\iota}\right)^2 - \delta_{11}(\alpha_{22} + \beta_{22}(0)) - \delta_{22}\alpha_{11}(0) + \delta_{12}N_2(0)\beta_{21}(0)\right)\left(\frac{n}{\iota}\right)^2\\
&\quad + \det(J(0; 0, 0)).
\end{aligned}$$

It is easy to check that $\mathrm{tr}(J(n; 0, 0)) < 0$ provided (H1) holds. Now we view $\det(J(n; 0, 0))$ as a quadratic function with respect to $\left(\frac{n}{\iota}\right)^2$. Denote

$$\Theta = \delta_{11}(\alpha_{22} + \beta_{22}(0)) + \delta_{22}\alpha_{11}(0) - \delta_{12}N_2(0)\beta_{21}(0). \tag{9}$$

Clearly, if $\Theta < 0$, then $\det(J(n; 0, 0)) > 0$, and if $\Theta > 0$, then $\det(J(n; 0, 0)) > 0$ provided that $\Delta < 0$, where

$$\Delta = (\delta_{11}(\alpha_{22} + \beta_{22}(0)) + \delta_{22}\alpha_{11}(0) - \delta_{12}N_2(0)\beta_{21}(0))^2 - 4\delta_{11}\delta_{22}\det(J(0; 0, 0)). \tag{10}$$

Besides (H1), we also make the following hypothesis:

(**H**2) $\Theta < 0$ or $\Theta > 0$ and $\Delta < 0$.

Under assumptions (H1)-(H2), $E_2(0)$ is always stable for model (2) without delays. In the sequel of this paper, we always assume that (H1) and (H2) both hold and are mainly concerned with the conditions for the occurrence of Hopf bifurcations around $E_2(\sigma)$ induced by delays.

3.2. Hopf bifurcations induced by maturation delay when $n = 0$

When $n = 0$, the characteristic equation (8) becomes

$$\mathfrak{g}_0^0(\lambda, \sigma) + \mathfrak{g}_1^0(\lambda, \sigma)\mathrm{e}^{-\lambda\sigma} = 0, \tag{11}$$

which meets the requirements in [17]. By plugging $\lambda = i\chi^0 (\chi^0 > 0)$ into Eq. (11), we obtain

$$\begin{cases}
\Re\left(\mathfrak{g}_1^0(i\chi^0, \sigma)\right)\cos(\chi^0\sigma) + \Im\left(\mathfrak{g}_1^0(i\chi^0, \sigma)\right)\sin(\chi^0\sigma) = -\Re\left(\mathfrak{g}_0^0(i\chi^0, \sigma)\right),\\
\Im\left(\mathfrak{g}_1^0(i\chi^0, \sigma)\right)\cos(\chi^0\sigma) - \Re\left(\mathfrak{g}_1^0(i\chi^0, \sigma)\right)\sin(\chi^0\sigma) = -\Im\left(\mathfrak{g}_0^0(i\chi^0, \sigma)\right).
\end{cases} \tag{12}$$

From Eq. (12) we can solve that

$$\begin{cases} \cos\chi^0\sigma = -\frac{\Re(\mathfrak{g}_0^0(i\chi^0,\sigma))\Re(\mathfrak{g}_1^0(i\chi^0,\sigma))+\Im(\mathfrak{g}_0^0(i\chi^0,\sigma))\Im(\mathfrak{g}_1^0(i\chi^0,\sigma))}{(\Re(\mathfrak{g}_1^0(i\chi^0,\sigma)))^2+(\Im(\mathfrak{g}_1^0(i\chi^0,\sigma)))^2}, \\ \sin\chi^0\sigma = -\frac{\Re(\mathfrak{g}_0^0(i\chi^0,\sigma))\Im(\mathfrak{g}_1^0(i\chi^0,\sigma))-\Re(\mathfrak{g}_1^0(i\chi^0,\sigma))\Im(\mathfrak{g}_0^0(i\chi^0,\sigma))}{(\Re(\mathfrak{g}_1^0(i\chi^0,\sigma)))^2+(\Im(\mathfrak{g}_1^0(i\chi^0,\sigma)))^2}. \end{cases} \tag{13}$$

It is direct from (13) that

$$G(\chi^0,\sigma) = (\chi^0)^4 + q_1^0(\sigma)(\chi^0)^2 + q_2^0(\sigma) = 0, \tag{14}$$

where

$$\begin{cases} q_1^0(\sigma) = \left(\mathfrak{g}_{01}^0(\sigma)\right)^2 - \left(\mathfrak{g}_{11}^0(\sigma)\right)^2 - 2\mathfrak{g}_{00}^0(\sigma), \\ q_2^0(\sigma) = (\mathfrak{g}_{10}^0(\sigma) + \mathfrak{g}_{00}^0(\sigma))(\mathfrak{g}_{00}^0(\sigma) - \mathfrak{g}_{10}^0(\sigma)). \end{cases}$$

Obviously, when $(q_1^0(\sigma))^2 - 4q_2^0(\sigma) > 0$, Eq. (14) may admit two real roots $\chi_\pm^0(\sigma)$ satisfying

$$(\chi_\pm^0(\sigma))^2 = \frac{-q_1^0(\sigma) \pm \sqrt{(q_1^0(\sigma))^2 - 4q_2^0(\sigma)}}{2}.$$

Assume that $\mathrm{Ad} \subseteq \mathbb{R}^+$ is the set of σ such that $\chi(\sigma)$ is a positive real root of Eq. (14). We can then find a $\theta(\sigma) \in [0,\pi)$ satisfying the following equations:

$$\begin{cases} \cos\theta(\sigma) = -\frac{\Re(\mathfrak{g}_0^0(i\chi(\sigma),\sigma))\Re(\mathfrak{g}_1^0(i\chi(\sigma),\sigma))+\Im(\mathfrak{g}_0^0(i\chi(\sigma),\sigma))\Im(\mathfrak{g}_1^0(i\chi(\sigma),\sigma))}{(\Re(\mathfrak{g}_1^0(i\chi(\sigma),\sigma)))^2+(\Im(\mathfrak{g}_1^0(i\chi(\sigma),\sigma)))^2}, \\ \sin\theta(\sigma) = -\frac{\Re(\mathfrak{g}_0^0(i\chi(\sigma),\sigma))\Im(\mathfrak{g}_1^0(i\chi(\sigma),\sigma))-\Re(\mathfrak{g}_1^0(i\chi(\sigma),\sigma))\Im(\mathfrak{g}_0^0(i\chi(\sigma),\sigma))}{(\Re(\mathfrak{g}_1^0(i\chi(\sigma),\sigma)))^2+(\Im(\mathfrak{g}_1^0(i\chi(\sigma),\sigma)))^2}. \end{cases}$$

Now denote $\sigma_k(\sigma)$ by

$$\sigma_k(\sigma) = \frac{\theta(\sigma) + 2k\pi}{\chi(\sigma)},\ k \in \mathbf{N}_0.$$

Then we can define the smooth functions $\mathcal{S}_k(\sigma)$ by

$$\mathcal{S}_k(\sigma) = \sigma - \sigma_k(\sigma),\ k \in \mathbf{N}_0.$$

According to Theorem 4.1 in [17], we can directly obtain the following theorem on the occurrence of Hopf bifurcations induced by maturation delay σ.

Theorem 2. *Eq. (11) has a pair of simply imaginary roots $\lambda = \pm i\chi(\sigma)$ for $\sigma \in \mathrm{Ad}$ provided that $\mathcal{S}_k(\sigma) = 0$ holds for some $k \in \mathbf{N}_0$. Besides, if $\chi(\sigma) = \chi_+^0(\sigma)$, then the corresponding pair eigenvalues cross the imaginary axis from left (right) to right (left) if $D_+(\sigma) > 0 (< 0)$; while if $\chi(\sigma) = \chi_-^0(\sigma)$, then the corresponding pair eigenvalues cross the imaginary axis from left (right) to right (left) if $D_-(\sigma) > 0 (< 0)$. Here,*

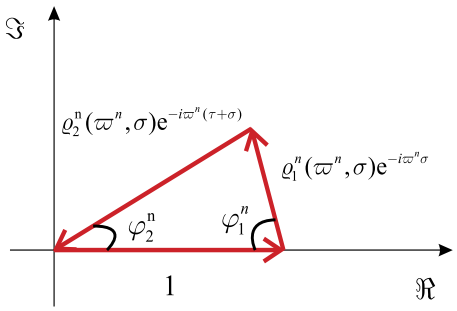

Fig. 1. Triangle constituted by $1, \varrho_1^n(\varpi^n,\sigma)e^{-i\varpi^n\sigma}, \varrho_2^n(\varpi^n,\sigma)e^{-i\varpi^n(\tau+\sigma)}$.

$$D_{\pm}(\sigma) := \mathrm{Sign}\left\{\frac{d\Re\lambda}{d\sigma}\Big|_{\lambda=i\chi_{\pm}^0(\sigma)}\right\} = \pm\mathrm{Sign}\left\{\frac{d\mathcal{S}_k(\sigma)}{d\sigma}\right\}.$$

3.3. *Crossing curve method to detect Hopf bifurcations when $n \neq 0$*

In this subsection, we generalize the methods used in [29,35,41,42] to obtain the stability crossing curves for spatial model (2) with delay-dependent parameters. Suppose $\lambda = i\varpi^n(\varpi^n > 0)$ is a root of Eq. (8) and notice that $\mathfrak{g}_0^n(i\varpi^n,\sigma) \neq 0$. Eq. (8) can be rewritten as

$$1 + \varrho_1^n(\varpi^n,\sigma)e^{-i\varpi^n\sigma} + \varrho_2^n(\varpi^n,\sigma)e^{-i\varpi^n(\tau+\sigma)} = 0, \tag{15}$$

where

$$\begin{cases} \varrho_1^n(\varpi^n,\sigma) = \dfrac{\mathfrak{g}_1^n(i\varpi^n,\sigma)}{\mathfrak{g}_0^n(i\varpi^n,\sigma)}, \\ \varrho_2^n(\varpi^n,\sigma) = \dfrac{\mathfrak{g}_2^n(\sigma)}{\mathfrak{g}_0^n(i\varpi^n,\sigma)}. \end{cases}$$

Notice that in the complex plane, the three items on the left of Eq. (15) constitute a triangle (see Fig. 1). Define

$$\begin{cases} \Upsilon_1^n = |\mathfrak{g}_0^n(\varpi^n,\sigma)| + |\mathfrak{g}_1^n(\varpi^n,\sigma)| - |\mathfrak{g}_2^n(\sigma)|, \\ \Upsilon_2^n = |\mathfrak{g}_0^n(\varpi^n,\sigma)| + |\mathfrak{g}_2^n(\sigma)| - |\mathfrak{g}_1^n(\varpi^n,\sigma)|, \\ \Upsilon_3^n = |\mathfrak{g}_1^n(\varpi^n,\sigma)| + |\mathfrak{g}_2^n(\sigma)| - |\mathfrak{g}_0^n(\varpi^n,\sigma)|, \end{cases} \tag{16}$$

and

$$\Omega_n = \{(\varpi^n,\sigma) : \Upsilon_i^n \geq 0, i = 1,2,3\}.$$

Then Ω_n is the feasible region of (ϖ^n,σ).

Obviously, we require that Ω_n is nonempty. Denote by $\varphi_1^n(\varpi^n,\sigma)$ and $\varphi_2^n(\varpi^n,\sigma)$ respectively as the angles constituted by 1 and $\varrho_1^n(\varpi^n,\sigma)e^{-i\varpi^n\sigma}$, and $\varrho_2^n(\varpi^n,\sigma)e^{-i\varpi^n(\tau+\sigma)}$ (see Fig. 1). It then follows from the law of cosine that

$$\begin{cases} \varphi_1^n(\varpi^n,\sigma) = \arccos\left[\frac{1+|\varrho_1^n(\varpi^n,\sigma)|^2-|\varrho_2^n(\varpi^n,\sigma)|^2}{2|\varrho_1^n(\varpi^n,\sigma)|}\right], \\ \varphi_2^n(\varpi^n,\sigma) = \arccos\left[\frac{1+|\varrho_2^n(\varpi^n,\sigma)|^2-|\varrho_1^n(\varpi^n,\sigma)|^2}{2|\varrho_2^n(\varpi^n,\sigma)|}\right]. \end{cases}$$

Notice that the sign of $\Im\,(\varrho_1^n(\varpi^n,\sigma)\mathrm{e}^{-i\varpi^n\sigma})$ does not alter for $(\varpi^n,\sigma)\in \mathrm{Int}\ \Omega_n^k$, where $\Omega_n^k, k=1,2,\cdots,K$ refer to connected region of Ω_n. Denote by $\mathcal{I}_{k,n}=[\varpi_{k,n}^l,\varpi_{k,n}^r]$ and $\mathcal{I}_{k,n}^{\varpi}=[\sigma_{k,n}^{\varpi,l},\sigma_{k,n}^{\varpi,r}]$ respectively the feasible set of ϖ^n and the feasible interval of σ for every $\varpi^n\in\mathcal{I}_{k,n}$. Thereupon, we discuss the two possible scenarios as follows.

(i) $\Im\,(\varrho_1^n(\varpi^n,\sigma)\mathrm{e}^{-i\varpi^n\sigma})>0$. In this scenario, we have

$$\begin{cases} \arg(\varrho_1^n(\varpi^n,\sigma)\mathrm{e}^{-i\varpi^n\sigma}) = \pi-\varphi_1^n(\varpi^n,\sigma), \\ \arg(\varrho_2^n(\varpi^n,\sigma)\mathrm{e}^{-i\varpi^n(\tau+\sigma)}) = \varphi_2^n(\varpi^n,\sigma)-\pi. \end{cases}$$

We then obtain

$$\arg(\varrho_1^n(\varpi^n,\sigma))-\varpi^n\sigma+2i\pi=\pi-\varphi_1^n(\varpi^n,\sigma),\ \text{for some } i\in\mathbb{Z},$$

and

$$\arg(\varrho_2^n(\varpi^n,\sigma))-\varpi^n(\tau+\sigma)+2j\pi=\varphi_2^n(\varpi^n,\sigma)-\pi,\ \text{for some } j\in\mathbb{Z}. \tag{17}$$

From (17) we obtain that

$$\tau=\frac{1}{\varpi^n}\big[\arg(\varrho_2^n(\varpi^n,\sigma))-\varpi^n\sigma+(2j+1)\pi-\varphi_2^n(\varpi^n,\sigma)\big].$$

(ii) $\Im\,(\varrho_1^n(\varpi^n,\sigma)\mathrm{e}^{-i\varpi^n\sigma})<0$. In this scenario, the triangle formed by 1, $\varrho_1^n(\varpi^n,\sigma)\mathrm{e}^{-i\varpi^n\sigma}$ and $\varrho_2^n(\varpi^n,\sigma)\mathrm{e}^{-i\varpi^n(\tau+\sigma)}$ is the mirror image of the one in Fig. 1 about the real axis. Arguing similarly to above, we obtain

$$\arg(\varrho_1^n(\varpi^n,\sigma))-\varpi^n\sigma+2i\pi=-\pi+\varphi_1^n(\varpi^n,\sigma),\ \text{for some } i\in\mathbb{Z},$$

and

$$\tau=\frac{1}{\varpi^n}\big[\arg(\varrho_2^n(\varpi^n,\sigma))-\varpi^n\sigma+(2j-1)\pi+\varphi_2^n(\varpi^n,\sigma)\big],\ \text{for some } j\in\mathbb{Z}.$$

Now define the functions $\mathcal{S}_\iota^{\pm},\iota\in\mathbb{Z}$ as

$$\mathcal{S}_\iota^{\pm}(\varpi^n,\sigma)=\sigma-\frac{1}{\varpi^n}\big[\arg(\varrho_1^n(\varpi^n,\sigma))+(2\iota-1)\pi\pm\varphi_1^n(\varpi^n,\sigma)\big],$$

and for fixed $\varpi^n\in\mathcal{I}_{k,n}$, denote by $\tilde{\sigma}^{m\pm}(\varpi^n)$ the positive roots of $\mathcal{S}_\iota^{\pm}=0$. Thereupon, we can define the admissible values of τ as

$$\tilde{\tau}_m^{\kappa\pm}(\varpi^n)=\frac{1}{\varpi^n}\big[\arg\big(\varrho_2^n(\varpi^n,\tilde{\sigma}^{m\pm}(\varpi^n))\big)-\varpi^n\tilde{\sigma}^{m\pm}(\varpi^n)+(2\kappa^{\pm}-1)\pi\mp\varphi_2^n(\varpi^n,\tilde{\sigma}^{m\pm})\big],$$

for $\kappa = \kappa_0^{\pm}, \kappa_0^{\pm}+1, \cdots$, where $\kappa_0^{\pm}$ refer to the smallest possible integers satisfying $\tilde{\tau}_m^{\kappa\pm}(\varpi^n) \geq 0$. Let $\mathcal{I}_n = \bigcup_k \mathcal{I}_{k,n}$. By taking all $\varpi^n \in \mathcal{I}_n$, we can then define the following curves:

$$C^n = \left\{(\varpi^n, \tilde{\sigma}^{m\pm}(\varpi^n)) : \varpi^n \in \mathcal{I}_n, \mathcal{S}_\iota^{\pm}(\varpi^n, \tilde{\sigma}^{m\pm}(\varpi^n)) = 0\right\}.$$

Thus we obtain the stability crossing curves:

$$\mathcal{T}^n = \left\{(\tilde{\sigma}^{m\pm}(\varpi^n), \tilde{\tau}_m^{\kappa\pm}(\varpi^n)) : \varpi^n \in \mathcal{I}_n, \mathcal{S}_\iota^{\pm}(\varpi^n, \tilde{\sigma}^{m\pm}(\varpi^n)) = 0\right\}.$$

We further make the following hypothesis to ensure the crossing curves can be extended.

(**H**3) $\dfrac{\partial \mathcal{S}_\iota^{\pm}(\varpi^n, \sigma)}{\partial \sigma} \neq 0$ for $(\varpi^n, \sigma) \in C^n$.

Hence, the categories of crossing curves are similar as given by [35].

Moreover, to assure the occurrence of Hopf bifurcations, we need further determine the direction in which the root of Eq. (8) crosses the imaginary axis as (σ, τ) passes through a crossing curve $\mathcal{T}^n$. By applying the results in [35], we have the following result.

Theorem 3. *Assume that Eq. (8) has a pair of purely imaginary roots $\pm i\varpi_0^n$ for $(\sigma, \tau) = (\sigma_0^n, \tau_0^n) \in \mathcal{T}^n$. Then Eq. (8) has a pair of conjugate complex roots $\lambda_{\pm}^n(\sigma, \tau) = \alpha^n(\sigma, \tau) \pm i\varpi^n(\sigma, \tau)$ around (σ_0^n, τ_0^n) with $\alpha^n(\sigma_0^n, \tau_0^n) = 0$ and $\varpi^n(\sigma_0^n, \tau_0^n) = \varpi_0^n$. Additionally, $\lambda_{\pm}^n(\sigma, \tau)$ passes through the imaginary axis from left to right as (σ, τ) passes through the crossing curve to the region on the right (left) whenever $\mathcal{D}(\lambda, \tau, \sigma)\big|_{(\lambda,\tau,\sigma)=(i\varpi_0^n, \tau_0^n, \sigma_0^n)} > 0$ (< 0), where*

$$\mathcal{D}(\lambda, \tau, \sigma) = -\Re\left\{\left[\frac{\partial \mathfrak{g}_0^n}{\partial \sigma} e^{\lambda(\tau+\sigma)} + \left(\frac{\partial \mathfrak{g}_1^n}{\partial \sigma} - \lambda \mathfrak{g}_1^n\right) e^{\lambda\tau} + \left(\frac{\partial \mathfrak{g}_2^n}{\partial \sigma} - \lambda \mathfrak{g}_2^n\right)\right] \overline{\mathfrak{g}_2^n}\right\}.$$

Here the left (right) region of a crossing curve refers to the region on the left-hand (right-hand) side when one moves along the positive direction (in which ϖ^n increases) of the curve.

Remark 2. In fact, the crossing curves $\mathcal{T}^n$ exist only for finite n. This can be easily seen by noting that in (16), $\Upsilon_3^n < 0$ when n is large enough.

4. Direction and stability of Hopf bifurcation

From the above discussions, we have known that for fixed maturation delay σ in its stable intervals, there exist n_H and τ_H^n such that (i) Eq. (8) admits a pair of conjugate complex roots $i\varpi_H^n$ and all other eigenvalues have negative real parts, and moreover (ii) the transversality condition is satisfied. That is model (2) undergoes a Hopf bifurcation at $\tau = \tau_H^n$. In this section, by generalizing the method set forth in [34,36] to model (2) with delay-dependent parameters, we will calculate the normal form of Hopf bifurcation at $E_2(\sigma)$ to further determine the properties of bifurcating periodic solutions.

4.1. Notations and equation transformation

We first present some convention notations used in [34,36]. For the simplify of notation, we denote $E_2(\sigma) = (N_2(\sigma), P_2(\sigma))$ by $E_2(N_2, P_2)$, and denote for fixed n, the Hopf bifurcation point τ_H^n and frequency ϖ_H^n respectively by τ_H and ϖ_H. We further define the following real-valued Hilbert space:

$$\aleph = \left\{ \mathcal{V} = (\mathcal{V}_1, \mathcal{V}_2) \in H^2(0, \iota\pi) \oplus H^2(0, \iota\pi) : \left. \frac{\partial \mathcal{V}_1}{\partial x} \right|_{x=0,\iota\pi} = \left. \frac{\partial \mathcal{V}_2}{\partial x} \right|_{x=0,\iota\pi} = 0 \right\},$$

endowed with the following inner product:

$$[\mathcal{U}, \mathcal{V}] = \int_0^{\iota\pi} \mathcal{U}^{\mathrm{T}} \mathcal{V} \mathrm{d}x, \text{ for } \mathcal{U}, \mathcal{V} \in \aleph.$$

Denote $\mathcal{C} = C([-\max\{1, \frac{\sigma}{\tau}\}, 0]; \aleph)$ as functional space consisted of continuous mappings from $[-\max\{1, \frac{\sigma}{\tau}\}, 0]$ to $\aleph$ with the usual supremum norm. Denote

$$b_n(x) = \frac{\cos \frac{n}{\iota} x}{||\cos \frac{n}{\iota} x||_{L^2}} = \begin{cases} \sqrt{\frac{1}{\iota\pi}}, & n = 0, \\ \sqrt{\frac{2}{\iota\pi}} \cos\left(\frac{nx}{\iota}\right), & n \geq 1. \end{cases}$$

Let $\beta_n^{(1)} = (b_n, 0)^{\mathrm{T}}$, $\beta_n^{(2)} = (0, b_n)^{\mathrm{T}}$. Denote $\tau = \tau_H + \zeta$, $|\zeta| \ll 1$ as the small perturbation of τ_H such that $\zeta = 0$ is the Hopf bifurcation point for model (2) with fixed maturation delay σ. Moreover, ζ is regarded as a state variable in the following computation. Also, let

$$\mathfrak{B}(\alpha\omega_1^{\vartheta_1}\omega_2^{\vartheta_2}\zeta) = \begin{pmatrix} \alpha\omega_1^{\vartheta_1}\omega_2^{\vartheta_2}\zeta \\ \overline{\alpha}\omega_1^{\vartheta_2}\omega_2^{\vartheta_1}\zeta \end{pmatrix}, \alpha \in \mathbb{C}.$$

We then make the following transformation to shift E_2 to the origin and normalize the memory delay τ:

$$\begin{aligned} v_1(t, x) &= N(\tau t, x) - N_2, \\ v_2(t, x) &= P(\tau t, x) - P_2. \end{aligned}$$

Let $\mathcal{V} = (v_1, v_2)^{\mathrm{T}}$. We write $\mathcal{V}(x, t)$ and $\mathcal{V}_t(\rho) = \mathcal{V}(x, t + \rho)$, $-\max\{1, \frac{\sigma}{\tau}\} \leq \rho \leq 0$ as $\mathcal{V}(t)$ and $\mathcal{V}_t \in \aleph$ respectively. Then model (2) can be rewritten as the following form:

$$\frac{\mathrm{d}\mathcal{V}(t)}{\mathrm{d}t} = \delta(\zeta)(\mathcal{V}_t)_{xx} + \mathfrak{L}(\zeta)\mathcal{V}_t + \mathfrak{F}(\mathcal{V}_t, \zeta), \tag{18}$$

where for $\psi = (\psi^{(1)}, \psi^{(2)})^{\mathrm{T}} \in \mathcal{C}$, $\delta(\zeta)(\cdot)_{xx}$ is described by

$$\delta(\zeta)(\psi)_{xx} = \delta_0(\psi)_{xx} + \mathfrak{F}^d(\psi, \zeta),$$

with

$$
\begin{aligned}
\delta_0(\psi)_{xx} &= \tau_H \begin{pmatrix} \delta_{11} & 0 \\ 0 & \delta_{22} \end{pmatrix} \begin{pmatrix} \psi_{xx}^{(1)}(0) \\ \psi_{xx}^{(2)}(0) \end{pmatrix} + \tau_H \begin{pmatrix} 0 & \delta_{12}N_2 \\ 0 & 0 \end{pmatrix} \begin{pmatrix} \psi_{xx}^{(1)}(-1) \\ \psi_{xx}^{(2)}(-1) \end{pmatrix} \\
&:= \tau_H D_1 \psi_{xx}(0) + \tau_H D_2 \psi_{xx}(-1), \\
\mathfrak{F}^d(\psi,\zeta) &= \delta_{12}(\tau_H+\zeta) \begin{pmatrix} \psi_x^{(1)}(0)\psi_x^{(2)}(-1) + \psi^{(1)}(0)\psi_{xx}^{(2)}(-1) \\ 0 \end{pmatrix} \\
&\quad + \zeta \begin{pmatrix} \delta_{11}\psi_{xx}^{(1)}(0) + \delta_{12}N_2\psi_{xx}^{(2)}(-1) \\ \delta_{22}\psi_{xx}^{(2)}(0) \end{pmatrix},
\end{aligned} \tag{19}
$$

and $\mathfrak{L}(\zeta)$ is defined by

$$
\begin{aligned}
&\mathfrak{L}(\zeta)(\psi) \\
&= (\tau_H+\zeta)\left(\begin{pmatrix} \alpha_{11}(\sigma) & \alpha_{12}(\sigma) \\ 0 & \alpha_{22} \end{pmatrix} \begin{pmatrix} \psi^{(1)}(0) \\ \psi^{(2)}(0) \end{pmatrix} + \begin{pmatrix} 0 & 0 \\ \beta_{21}(\sigma) & \beta_{22}(\sigma) \end{pmatrix} \begin{pmatrix} \psi^{(1)}(-\frac{\sigma}{\tau_H+\zeta}) \\ \psi^{(2)}(-\frac{\sigma}{\tau_H+\zeta}) \end{pmatrix} \right) \\
&:= (\tau_H+\zeta)\left(A_1\psi(0) + A_2\psi(-\tilde{\sigma})\right).
\end{aligned}
$$

Furthermore, $\mathfrak{F}(\psi,\zeta)$ is given by

$$
\mathfrak{F}(\psi,\zeta) = (\tau_H+\zeta) \begin{pmatrix} f\left(\psi^{(1)}(0)+N_2, \psi^{(2)}(0)+P_2\right) \\ g\left(\psi^{(2)}(0)+P_2, \psi^{(1)}(-\tilde{\sigma})+N_2, \psi^{(2)}(-\tilde{\sigma})+P_2\right) \end{pmatrix} - \mathfrak{L}(\zeta)(\psi). \tag{20}
$$

By extracting the linear parts from the nonlinear parts, we can rewrite (18) as

$$
\frac{\mathrm{d}\mathcal{V}(t)}{\mathrm{d}t} = \delta_0(\mathcal{V}_t)_{xx} + \mathcal{L}_0(\mathcal{V}_t) + \widetilde{\mathfrak{F}}(V_t,\zeta), \tag{21}
$$

where $\mathcal{L}_0(\psi) = \tau_H\left(A_1\psi(0) + A_2\psi(-\hat{\sigma})\right)$, $\hat{\sigma} = \frac{\sigma}{\tau_H}$ and

$$
\widetilde{\mathfrak{F}}(\psi,\zeta) = \mathfrak{L}(\zeta)(\psi) - \mathcal{L}_0(\psi) + \mathfrak{F}(\psi,\zeta) + \mathfrak{F}^d(\psi,\zeta). \tag{22}
$$

Then we can obtain the linear system of Eq. (21) as

$$
\frac{\mathrm{d}\mathcal{V}_t}{\mathrm{d}t} = \delta_0(\mathcal{V}_t)_{xx} + \mathcal{L}_0(\mathcal{V}_t). \tag{23}
$$

We further choose the following enlarged space to rewrite (21) as an abstract ordinary differential equation in a Banach space [43,44]:

$$
\mathfrak{BC} := \left\{ \Psi \,\middle|\, \Psi \in C([-\max\{1,\frac{\sigma}{\tau}\},0),\aleph), \exists \lim_{\rho\to 0^-} \Psi(\rho) \in \aleph \right\}.
$$

Then Eq. (21) is equivalent to

$$
\frac{\mathrm{d}\mathcal{V}_t}{\mathrm{d}t} = \widetilde{J}\mathcal{V}_t + Y_0\widetilde{\mathfrak{F}}(\psi,\zeta). \tag{24}
$$

Here, $\widetilde{J}$ is a linear operator from $\mathcal{C}_0^1 = \{\psi \in \mathcal{C} \Big| \ \dot{\psi} \in \mathcal{C}, \psi(0) \in \mathrm{dom}((\cdot)_{xx})\}$ to $\mathfrak{BC}$, which is formulated by

$$\widetilde{J}\psi = \dot{\psi} + Y_0\Big(\tau_H D_1 \psi_{xx}(0) + \tau_H D_2 \psi_{xx}(-1) + \mathcal{L}_0(\psi) - \dot{\psi}(0)\Big),$$

and $Y_0 = Y_0(\rho)$ is formulated by

$$Y_0(\rho) = \begin{cases} 0, & \rho \in [-\max\{1, \frac{\sigma}{\tau}\}, 0), \\ 1, & \rho = 0. \end{cases}$$

Thereupon, we employ the method set forth in [43] to decompose $\mathfrak{BC}$. Let $\mathcal{C}_2 := C([-\max\{1, \frac{\sigma}{\tau}\}, 0]; \mathbb{R}^2)$, $\mathcal{C}_2^* := C([0, \max\{1, \frac{\sigma}{\tau}\}]; \mathbb{R}^{2*})$, and adopt the following adjoint bilinear form on $\mathcal{C}_2^* \times \mathcal{C}_2$:

$$\langle \mathcal{Q}(s), \mathcal{P}(\rho)\rangle = \mathcal{Q}(0)\mathcal{P}(0) - \int_{-\max\{1, \frac{\sigma}{\tau}\}}^{0} \int_{\xi=0}^{\rho} \mathcal{Q}(\xi - \rho)\mathrm{d}\Theta_n(\rho)\mathcal{P}(\xi)\mathrm{d}\xi, \ \text{for } \mathcal{Q} \in \mathcal{C}^*, \mathcal{P} \in \mathcal{C},$$

where $\Theta_n(\rho) \in BV([-\max\{1, \frac{\sigma}{\tau}\}, 0]; \mathbb{R}^{2\times 2})$, such that for $P(\rho) \in \mathcal{C}_2$, we have

$$-\tau_H(\frac{n_H}{\iota})^2 D_1 \mathcal{P}_{xx}(0) - \tau_H(\frac{n_H}{\iota})^2 D_2 \mathcal{P}_{xx}(-1) + \mathfrak{L}_0(\mathcal{P}(\rho)) = \int_{-\max\{1, \frac{\sigma}{\tau}\}}^{0} \mathrm{d}\Theta_n(\rho)\mathcal{P}(\rho).$$

Let $\mathcal{P}(\rho) = (p(\rho), \overline{p}(\rho))$, $\mathcal{Q}(s) = (q^{\mathrm{T}}(s), \overline{q}^{\mathrm{T}}(s))^{\mathrm{T}}$, where $p(\rho) = (p_1(\rho), p_2(\rho))^{\mathrm{T}} = p\mathrm{e}^{i\varpi_H\tau_H\rho}$ with $p = (p_1, p_2)^{\mathrm{T}}$ represents the corresponding eigenvector to $i\varpi_H\tau_H$ of (23), and $q(s) = (q_1(s), q_2(s))^{\mathrm{T}} = q\mathrm{e}^{-i\varpi_H\tau_H s}$ with $q = (q_1, q_2)^{\mathrm{T}}$ is the corresponding adjoint eigenvector of (23) meeting

$$\langle \mathcal{Q}(s), \mathcal{P}(\rho)\rangle = E_2.$$

Doing some algebra yields

$$p = \begin{pmatrix} 1 \\ \frac{-\beta_{21}(\sigma)\mathrm{e}^{-i\varpi_H\sigma}}{-\delta_{22}\left(\frac{n_H}{\iota}\right)^2 + \alpha_{22}(\sigma) + \beta_{22}(\sigma)\mathrm{e}^{-i\varpi_H\sigma} - i\varpi_H} \end{pmatrix}$$

and

$$q = \eta \begin{pmatrix} 1 \\ \frac{\delta_{11}\left(\frac{n_H}{\iota}\right)^2 - \alpha_{11}(\sigma) + i\varpi_H}{\beta_{21}(\sigma)\mathrm{e}^{-i\varpi_H\sigma}} \end{pmatrix},$$

where

$$\eta = \frac{k_2}{k_2 - k_1 + \tau_H \delta_{12} N_2 \left(\frac{n_H}{\iota}\right)^2 \beta_{21}(\sigma) \mathrm{e}^{-i\varpi_H(\sigma+\tau_H)} + k_1 k_2 \sigma - k_1 \sigma \beta_{22}(\sigma) \mathrm{e}^{-i\varpi_H \sigma}},$$

with $k_1 = \delta_{11}\left(\frac{n_H}{\iota}\right)^2 - \alpha_{11}(\sigma) + i\varpi_H$ and $k_2 = -\delta_{22}\left(\frac{n_H}{\iota}\right)^2 + \alpha_{22} + \beta_{22}(\sigma)\mathrm{e}^{-i\varpi_H\sigma} - i\varpi_H$.

Furthermore we see from [34,43,44] that $\mathfrak{BC}$ can be decomposed as

$$\mathfrak{BC} = \mathrm{Im}\pi \oplus \mathrm{Ker}\pi,$$

where for $\widetilde{\psi} \in \mathcal{C}$, we define the projection $\pi : \mathcal{C} \to \mathrm{Im}\pi$ as

$$\pi(\widetilde{\psi}) = \left(\mathcal{P}(\rho)\left\langle \mathcal{Q}(0), \begin{pmatrix} [\widetilde{\psi}(\cdot), \beta_{n_H}^{(1)}] \\ [\widetilde{\psi}(\cdot), \beta_{n_H}^{(2)}] \end{pmatrix} \right\rangle\right)^{\mathrm{T}} b_{n_H}(x). \tag{25}$$

Hence, we can decompose $\mathcal{V}_t(\rho)$ as

$$\begin{aligned} \mathcal{V}_t(\rho) &= \left(\mathcal{P}(\rho)\begin{pmatrix} \omega_1 \\ \omega_2 \end{pmatrix}\right)^{\mathrm{T}} \begin{pmatrix} \beta_{n_H}^{(1)} \\ \beta_{n_H}^{(2)} \end{pmatrix} + z \\ &= \left(\omega_1 p \mathrm{e}^{i\varpi_H\tau_H\rho} + \omega_2 \bar{p}\mathrm{e}^{-i\varpi_H\tau_H\rho}\right) b_{n_H}(x) + \begin{pmatrix} z^{(1)} \\ z^{(2)} \end{pmatrix} \\ &:= \mathcal{P}(\rho)\omega_x + z, \end{aligned}$$

where $z \in \mathcal{Q}^1 := \mathcal{C}_0^1 \cap \mathrm{Ker}\pi$. Thereupon, we can decompose system (24) as the following abstract ordinary differential equations on $\mathbb{R}^2 \times \mathrm{Ker}\pi$:

$$\begin{cases} \dot{\omega} = \mathfrak{D}\omega + \mathcal{Q}(0)\begin{pmatrix} [\tilde{\mathfrak{F}}(\mathcal{P}(\rho)\omega_x + z, \zeta), \beta_{n_H}^{(1)}] \\ [\tilde{\mathfrak{F}}(\mathcal{P}(\rho)\omega_x + z, \zeta), \beta_{n_H}^{(2)}] \end{pmatrix}, \\ \dot{z} = \mathcal{A}_{\mathcal{Q}^1} z + (I - \pi) Y_0(\rho) \tilde{\mathfrak{F}}(\mathcal{P}(\rho)\omega_x + z, \zeta), \end{cases} \tag{26}$$

where $\omega = (\omega_1, \omega_2)^{\mathrm{T}}$, $\mathfrak{D} = \mathrm{diag}\{i\varpi_H\tau_H, -i\varpi_H\tau_H\}$, and $\mathcal{A}_{\mathcal{Q}^1} : \mathcal{Q}^1 \to \mathrm{Ker}\pi$ is given by

$$\mathcal{A}_{\mathcal{Q}^1} z = \dot{z} + Y_0(\rho)\left(\tau_H D_1 z_{xx}(0) + \tau_H D_2 z_{xx}(-1) + \mathcal{L}_0(z) - \dot{z}(0)\right).$$

Now, we study the following Taylor expansions:

$$\begin{aligned} \mathfrak{L}(\zeta)(\psi) &= \sum_{\kappa \geq 1} \frac{1}{\kappa!} \mathfrak{L}_\kappa(\zeta)(\psi), \qquad \tilde{\mathfrak{F}}(\psi, \zeta) = \sum_{\kappa \geq 2} \frac{1}{\kappa!} \tilde{\mathfrak{F}}_\kappa(\psi, \zeta), \\ \mathfrak{F}(\psi, \zeta) &= \sum_{\kappa \geq 2} \frac{1}{\kappa!} \mathfrak{F}_\kappa(\psi, \zeta), \qquad \mathfrak{F}^d(\psi, \zeta) = \sum_{\kappa \geq 2} \frac{1}{\kappa!} \mathfrak{F}_\kappa^d(\psi, \zeta). \end{aligned}$$

We recall from (22) that

$$\tilde{\mathfrak{F}}_2(\psi, \zeta) = 2\zeta\left(A_1\psi(0) + A_2\psi\left(-\frac{\sigma}{\tau^H}\right) + \frac{\sigma}{\tau_H} A_2\psi'\left(-\frac{\sigma}{\tau_H}\right)\right) + \mathfrak{F}_2(\psi, \zeta) + \mathfrak{F}_2^d(\psi, \zeta), \tag{27}$$

and

$$\tilde{\mathfrak{F}}_\kappa(\psi,\zeta)=\mathfrak{L}_\kappa(\zeta)(\psi)+\mathfrak{F}_\kappa(\psi,\zeta)+\mathfrak{F}_\kappa^d(\psi,\zeta),\ \kappa=3,4,\cdots. \tag{28}$$

We then rewrite system (26) as

$$\begin{cases}\dot{\omega}=\mathfrak{D}\omega+\sum_{\kappa\geq 2}\frac{1}{\kappa!}f_\kappa^1(\omega,z,\zeta),\\ \dot{z}=\mathcal{A}_{\mathcal{Q}^1}z+\sum_{\kappa\geq 2}\frac{1}{\kappa!}f_\kappa^2(\omega,z,\zeta),\end{cases} \tag{29}$$

where

$$\begin{cases}f_\kappa^1(\omega,z,\zeta)=\mathcal{Q}(0)\begin{pmatrix}[\tilde{\mathfrak{F}}_\kappa(\mathcal{P}(\rho)\omega_x+z,\zeta),\beta_{n_H}^{(1)}]\\ [\tilde{\mathfrak{F}}_\kappa(\mathcal{P}(\rho)\omega_x+z,\zeta),\beta_{n_H}^{(2)}]\end{pmatrix},\\ f_\kappa^2(\omega,z,\zeta)=(I-\pi)Y_0(\rho)\tilde{\mathfrak{F}}_\kappa(\mathcal{P}(\rho)\omega_x+z,\zeta).\end{cases} \tag{30}$$

By appealing to the following the change of variables [34,43]:

$$(\omega,z)=(\tilde{\omega},\tilde{z})+\frac{1}{\kappa!}\left(\mathcal{V}_\kappa^1(\tilde{\omega},\zeta),\mathcal{V}_\kappa^2(\tilde{\omega},\zeta)\right),\ \kappa\geq 2, \tag{31}$$

we then obtain the normal form of system (29) as below:

$$\dot{\omega}=\mathfrak{D}\omega+\sum_{\kappa\geq 2}g_\kappa^1(\omega,0,\zeta).$$

Define $(M_j^1 p)(\omega,\zeta)=D_\omega p(\omega,\zeta)\mathfrak{D}\omega-\mathfrak{D}p(\omega,\zeta)$ and $(M_j^2 h)(\omega,\zeta)=D_\omega h(\omega,\zeta)\mathfrak{D}\omega-\mathcal{A}_{\mathcal{Q}^1}h(\omega,\zeta)$. We then utilize method in [34,36] to find

$$g_2^1(\omega,0,\zeta)=\mathrm{Proj}_{\ker(M_2^1)}f_2^1(\omega,0,\zeta),$$

and

$$g_3^1(\omega,0,\zeta)=\mathrm{Proj}_{\ker(M_3^1)}\tilde{f}_3^1(\omega,0,\zeta)=\mathrm{Proj}_S\tilde{f}_3^1(\omega,0,0)+O(\zeta^2|\omega|), \tag{32}$$

where $\tilde{f}_3^1(\omega,0,\zeta)$ refers to the cubic polynomial of (ω,ζ) under the transformation of (31). Moreover, $\tilde{f}_3^1(\omega,0,\zeta)$ can be determined by (32),

$$\ker(M_2^1)=\mathrm{Span}\left\{\begin{pmatrix}\zeta\omega_1\\0\end{pmatrix},\begin{pmatrix}0\\\zeta\omega_2\end{pmatrix}\right\},$$
$$\ker(M_3^1)=\mathrm{Span}\left\{\begin{pmatrix}\omega_1^2\omega_2\\0\end{pmatrix},\begin{pmatrix}\zeta^2\omega_1\\0\end{pmatrix},\begin{pmatrix}0\\\omega_1\omega_2^2\end{pmatrix},\begin{pmatrix}0\\\zeta^2\omega_2\end{pmatrix}\right\},$$

and

$$S\ =\mathrm{Span}\left\{\begin{pmatrix}\omega_1^2\omega_2\\0\end{pmatrix},\begin{pmatrix}0\\\omega_1\omega_2^2\end{pmatrix}\right\}. \tag{33}$$

4.2. Calculation of $g_j^1(\omega, 0, \zeta)$

Calculation of $g_2^1(\omega, 0, \zeta)$. We recall from (19) that

$$\mathfrak{F}_2^d(\psi, \zeta) = \mathfrak{F}_{20}^d(\psi) + \zeta\ \mathfrak{F}_{21}^d(\psi), \tag{34}$$

and

$$\mathfrak{F}_3^d(\psi, \zeta) = \zeta \mathfrak{F}_{31}^d(\psi),\ \mathfrak{F}_\kappa^d(\psi, \zeta) = (0, 0)^{\mathrm{T}}, \kappa = 4, 5, \cdots, \tag{35}$$

where

$$\begin{cases} \mathfrak{F}_{20}^d(\psi) = 2\delta_{12}\tau_H \begin{pmatrix} \psi_x^{(1)}(0)\psi_x^{(2)}(-1) + \psi^{(1)}(0)\psi_{xx}^{(2)}(-1) \\ 0 \end{pmatrix}, \\ \mathfrak{F}_{21}^d(\psi) = 2D_1\psi_{xx}(0) + 2D_2\psi_{xx}(-1), \\ \mathfrak{F}_{31}^d(\psi) = 6\delta_{12} \begin{pmatrix} \psi_x^{(1)}(0)\psi_x^{(2)}(-1) + \psi^{(1)}(0)\psi_{xx}^{(2)}(-1) \\ 0 \end{pmatrix}. \end{cases} \tag{36}$$

Furthermore, it is fairly easy to obtain

$$\begin{aligned} &\begin{pmatrix} [2\zeta \left(A_1(\mathcal{P}(0)\omega_x) + A_2(\mathcal{P}(-\hat{\sigma})\omega_x) + \frac{\sigma}{\tau_H}A_2(\mathcal{P}'(-\hat{\sigma})\omega_x)\right), \beta_{n_H}^{(1)}] \\ [2\zeta \left(A_1(\mathcal{P}(0)\omega_x) + A_2(\mathcal{P}(-\hat{\sigma})\omega_x) + \frac{\sigma}{\tau_H}A_2(\mathcal{P}'(-\hat{\sigma})\omega_x)\right), \beta_{n_H}^{(2)}] \end{pmatrix} \\ &= 2\zeta \left(A_1\mathcal{P}(0) + (1 + i\varpi_H\sigma)A_2\mathcal{P}(-\hat{\sigma})\right) \begin{pmatrix} \omega_1 \\ \omega_2 \end{pmatrix}, \end{aligned} \tag{37}$$

$$\begin{pmatrix} [\zeta\mathfrak{F}_{21}^d(\mathcal{P}(\rho)\omega_x), \beta_{n_H}^{(1)}] \\ [\zeta\mathfrak{F}_{21}^d(\mathcal{P}(\rho)\omega_x), \beta_{n_H}^{(2)}] \end{pmatrix} = -2\left(\frac{n_H}{\iota}\right)^2 \zeta \left(D_1\left(\mathcal{P}(0)\begin{pmatrix} \omega_1 \\ \omega_2 \end{pmatrix}\right) + D_2\left(\mathcal{P}(-1)\begin{pmatrix} \omega_1 \\ \omega_2 \end{pmatrix}\right)\right), \tag{38}$$

and for all $\zeta \in \mathbb{R}$, $\mathfrak{F}_2(\mathcal{P}(\rho)\omega_x, \zeta) = \mathfrak{F}_2(\mathcal{P}(\rho)\omega_x, 0)$. Then (30) implies that

$$f_2^1(\omega, 0, \zeta) = \mathcal{Q}(0) \begin{pmatrix} [\tilde{\mathfrak{F}}_2(\mathcal{P}(\rho)\omega_x, \zeta), \beta_{n_H}^{(1)}] \\ [\tilde{\mathfrak{F}}_2(\mathcal{P}(\rho)\omega_x, \zeta), \beta_{n_H}^{(2)}] \end{pmatrix}. \tag{39}$$

This, together with (34), (35) and (37)-(39), leads to

$$g_2^1(\omega, 0, \zeta) = \mathrm{Proj}_{\ker(M_2^1)} f_2^1(\omega, 0, \zeta) = \mathfrak{B}(B_1\zeta\omega_1), \tag{40}$$

where

$$B_1 = 2q^{\mathrm{T}} \left(A_1 p(0) + A_2 p(-\hat{\sigma})(1 + i\varpi_H\sigma) - \left(\frac{n_H}{\iota}\right)^2 (D_1 p(0) + D_2 p(-1))\right).$$

Calculation of $g_3^1(z,0,\zeta)$. Denote

$$f_2^{(1,1)}(\omega,z,0)=\mathcal{Q}(0)\begin{pmatrix}[\mathfrak{F}_2(\mathcal{P}(\rho)\omega_x+z,0),\beta_{n_H}^{(1)}]\\ [\mathfrak{F}_2(\mathcal{P}(\rho)\omega_x+z,0),\beta_{n_H}^{(2)}]\end{pmatrix}, \tag{41}$$

and

$$f_2^{(1,2)}(\omega,z,0)=\mathcal{Q}(0)\begin{pmatrix}[\mathfrak{F}_2^d(\mathcal{P}(\rho)\omega_x+z,0),\beta_{n_H}^{(1)}]\\ [\mathfrak{F}_2^d(\mathcal{P}(\rho)\omega_x+z,0),\beta_{n_H}^{(2)}]\end{pmatrix}. \tag{42}$$

(40) implies that $g_2^1(\omega,0,0)=(0,0)^{\mathrm{T}}$. Then $\tilde{f}_3^1(\omega,0,0)$ is formulated by

$$\begin{aligned}\tilde{f}_3^1(\omega,0,0)=\quad & f_3^1(\omega,0,0)+\tfrac{3}{2}\Big[(D_\omega f_2^1(\omega,0,0))\mathcal{U}_2^1(\omega,0)+\Big(D_z f_2^{(1,1)}(\omega,0,0)\Big)\mathcal{U}_2^2(\omega,0)(\rho)\\ & +\Big(D_{z,z_x,z_{xx}} f_2^{(1,2)}(\omega,0,0)\Big)\mathcal{U}_2^{(2,d)}(\omega,0)(\rho)\Big],\end{aligned}$$

where $f_2^1(\omega,0,0)=f_2^{(1,1)}(\omega,0,0)+f_2^{(1,2)}(\omega,0,0)$,

$$\begin{aligned}D_{z,z_x,z_{xx}} f_2^{(1,2)}(\omega,0,0)=&\Big(D_z f_2^{(1,2)}(\omega,0,0),D_{z_x} f_2^{(1,2)}(\omega,0,0),D_{z_{xx}} f_2^{(1,2)}(\omega,0,0)\Big),\\ \mathcal{U}_2^1(\omega,0)=&(M_2^1)^{-1}\mathrm{Proj}_{Im(M_2^1)} f_2^1(\omega,0,0),\\ \mathcal{U}_2^2(\omega,0)=&(M_2^2)^{-1} f_2^2(\omega,0,0),\end{aligned} \tag{43}$$

and

$$\mathcal{U}_2^{(2,d)}(\omega,0)(\rho)=\Big(U_2^2(\omega,0)(\rho),U_{2x}^2(\omega,0)(\rho),U_{2xx}^2(\omega,0)(\rho)\Big)^{\mathrm{T}}. \tag{44}$$

We next finish the calculation of $\mathrm{Proj}_S\tilde{f}_3^1(\omega,0,0)$ in four steps.

Step 1. The calculation of $\mathrm{Proj}_S f_3^1(\omega,0,0)$

Define

$$\mathfrak{F}_3(\mathcal{P}(\rho)\omega_x,0)=\sum_{\vartheta_1+\vartheta_2=3}\Psi_{\vartheta_1\vartheta_2}\omega_1^{\vartheta_1}\omega_2^{\vartheta_2}b_{n_H}^3(x),\ \ \vartheta_1,\ \ \vartheta_2\in\mathbf{N}_0. \tag{45}$$

It follows from (28) and (35) that $\tilde{\mathfrak{F}}_3(\mathcal{P}(\rho)\omega_x,0)=\mathfrak{F}_3(\mathcal{P}(\rho)\omega_x,0)$. We then deduce from (30) and (45) that

$$f_3^1(\omega,0,0)=\mathcal{Q}(0)\left(\sum_{\vartheta_1+\vartheta_2=3}\Psi_{\vartheta_1\vartheta_2}\omega_1^{\vartheta_1}\omega_2^{\vartheta_2}\int_0^{\iota\pi}b_{n_H}^4(x)\mathrm{d}x\right),$$

which, together with $\int_0^{\iota\pi}b_{n_H}^4(x)\mathrm{d}x=\frac{3}{2\iota\pi}$, yields

$$\mathrm{Proj}_S f_3^1(\omega,0,0)=\mathfrak{B}(B_{21}\omega_1^2\omega_2),$$

where

$$B_{21}=\frac{3}{2\iota\pi}q^{\mathrm{T}}\Psi_{21}.$$

Step 2. The calculation of $\mathrm{Proj}_S((D_\omega f_2^1(\omega,0,0))\mathcal{U}_2^1(\omega,0))$
From (27) and (34) we have that

$$\tilde{\mathfrak{F}}_2(\mathcal{P}(\rho)\omega_x,0)=\mathfrak{F}_2(\mathcal{P}(\rho)\omega_x,0)+\mathfrak{F}_{20}^d(\mathcal{P}(\rho)\omega_x). \tag{46}$$

(20) implies

$$\begin{aligned}\mathfrak{F}_2(\mathcal{P}(\rho)\omega_x+z,\zeta)&=\mathfrak{F}_2(\mathcal{P}(\rho)\omega_x+z,0)\\&=b_{n_H}^2(x)\left(\sum_{\vartheta_1+\vartheta_2=2}\Psi_{\vartheta_1\vartheta_2}\omega_1^{\vartheta_1}\omega_2^{\vartheta_2}\right)+\mathcal{S}_2(\mathcal{P}(\rho)\omega_x,z)+O(|z|^2),\end{aligned} \tag{47}$$

where $\mathcal{S}_2(\Phi(\rho)\omega_x,z)$ refers to the product of $\mathcal{P}(\rho)\omega_x$ and z. In conjunction with (34) and (36), we have

$$\mathfrak{F}_2^d(\mathcal{P}(\rho)\omega_x,0)=\mathfrak{F}_{20}^d(\mathcal{P}(\rho)\omega_x)=\left(\tfrac{n_H}{\iota}\right)^2\left(\eta_{n_H}^2(x)-b_{n_H}^2(x)\right)\left(\textstyle\sum_{\vartheta_1+\vartheta_2=2}\Psi_{\vartheta_1\vartheta_2}^d\omega_1^{\vartheta_1}\omega_2^{\vartheta_2}\right), \tag{48}$$

where

$$\eta_{n_H}(x)=\frac{\sqrt{2}}{\sqrt{\iota\pi}}\sin\left(\frac{n_H x}{\iota}\right)$$

and

$$\begin{cases}\Psi_{20}^d=2\delta_{12}\tau_0\begin{pmatrix}p_1(0)p_2(-1)\\0\end{pmatrix}=\overline{\Psi_{02}^d},\\ \Psi_{11}^d=2\delta_{12}\tau_0\begin{pmatrix}2\Re\{\overline{p}_1(0)p_2(-1)\}\\0\end{pmatrix}.\end{cases} \tag{49}$$

It then follows from $\int_0^{\iota\pi}\eta_{n_H}^2(x)b_{n_H}(x)\mathrm{d}x=\int_0^{\iota\pi}b_{n_H}^3(x)\mathrm{d}x=0$ that

$$f_2^1(\omega,0,0)=\mathcal{Q}(0)\begin{pmatrix}[\tilde{\mathfrak{F}}_2(\mathcal{P}(\rho)\omega_x,0),\beta_{n_H}^{(1)}]\\[\tilde{\mathfrak{F}}_2(\mathcal{P}(\rho)\omega_x,0),\beta_{n_H}^{(2)}]\end{pmatrix}=(0,0)^{\mathrm{T}}. \tag{50}$$

Hence, in conjunction with (33) and (50), we obtain

$$\mathrm{Proj}_S\left((D_\omega f_2^1(\omega,0,0))\mathcal{U}_2^1(\omega,0)\right)=\mathfrak{B}(B_{22}\omega_1^2\omega_2),$$

where

$$B_{22} = (0,0)^{\mathrm{T}}.$$

Step 3. The calculation of $\mathrm{Proj}_S((D_z f_2^{(1,1)}(\omega,0,0))\mathcal{U}_2^2(\omega,0)(\rho))$
Denote

$$\mathcal{U}_2^2(\omega,0)(\rho) = h(\rho,\omega) = \sum_{n\in\mathbf{N}_0} h_n(\rho,\omega) b_n(x),$$

where $h_n(\rho,\omega) = \sum_{\vartheta_1+\vartheta_2=2} \hbar_{n,\vartheta_1\vartheta_2}(\rho)\omega_1^{\vartheta_1}\omega_2^{\vartheta_2}$. We can derive from [34] that

$$\begin{aligned}
&\begin{pmatrix} [\mathcal{S}_2(\mathcal{P}(\rho)\omega_x, \sum_{n\in\mathbf{N}_0} h_n(\rho,\omega)b_n(x)), \beta_{n_H}^{(1)}] \\ [\mathcal{S}_2(\mathcal{P}(\rho)\omega_x, \sum_{n\in\mathbf{N}_0} h_n(\rho,\omega)b_n(x)), \beta_{n_H}^{(2)}] \end{pmatrix} \\
= \quad & \textstyle\sum_{n\in\mathbf{N}_0} H_n \left(\mathcal{S}_2(p(\rho)\omega_1, h_n(\rho,\omega)) + \mathcal{S}_2(\bar{p}(\rho)\omega_2, h_n(\rho,\omega))\right),
\end{aligned}$$

where

$$H_n = \int_0^{\iota\pi} b_{n_H}^2(x) b_n(x)\mathrm{d}x = \begin{cases} \frac{1}{\sqrt{\iota\pi}}, & n=0, \\ \frac{1}{\sqrt{2\iota\pi}}, & n=2n_H, \\ 0, & \text{otherwise.} \end{cases}$$

Hence, we have

$$\begin{aligned}
&(D_z f_2(1,1)(\omega,0,0))\mathcal{U}_2^2(\omega,0)(\rho) \\
=&\mathcal{Q}(0)\left(\sum_{n=0,n=2n_H} H_n\Big(\mathcal{S}_2(p(\rho)\omega_1, h_n(\rho,\omega)) + \mathcal{S}_2(\bar{p}(\rho)\omega_2, h_n(\rho,\omega))\Big)\right),
\end{aligned}$$

and

$$\mathrm{Proj}_S((D_z f_2^{(1,1)}(\omega,0,0))\mathcal{U}_2^2(\omega,0)(\rho)) = \mathfrak{B}(B_{23}\omega_1^2\omega_2),$$

where

$$\begin{aligned}
B_{23} =& \frac{1}{\sqrt{\iota\pi}} q^{\mathrm{T}} \left(\mathcal{S}_2(p(\rho), \hbar_{0,11}(\rho)) + \mathcal{S}_2(\bar{p}(\rho), \hbar_{0,20}(\rho))\right) \\
&+ \frac{1}{\sqrt{2\iota\pi}} q^{\mathrm{T}} \left(\mathcal{S}_2(p(\rho), \hbar_{2n_H,11}(\rho)) + \mathcal{S}_2(\bar{p}(\rho), \hbar_{2n_H,20}(\rho))\right).
\end{aligned}$$

Step 4. The calculation of $\mathrm{Proj}_S\left((D_{z,z_x,z_{xx}} f_2^{(1,2)}(\omega,0,0))\mathcal{U}_2^{(2,d)}(\omega,0)(\rho)\right)$

Let $\mathcal{V}(\rho)=(\mathcal{V}^{(1)},\mathcal{V}^{(2)})=\mathcal{P}(\rho)\omega_x$ and

$$\begin{aligned}\mathfrak{F}_2^d(\mathcal{V}(\rho),z,z_x,z_{xx})&=\mathfrak{F}_2^d(\mathcal{V}(\rho)+z,0)=F_{20}^d(\mathcal{V}(\rho)+z)\\&=2\delta_{12}\tau_H\begin{pmatrix}(\mathcal{V}^{(1)}(0)+z^{(1)}(0))(\mathcal{V}_{xx}^{(2)}(-1)+z_{xx}^{(2)}(-1))\\0\end{pmatrix}\\&\quad+2\delta_{12}\tau_H\begin{pmatrix}(\mathcal{V}_x^{(1)}(0)+w_x^{(1)}(0))(\mathcal{V}_x^{(2)}(-1)+z_x^{(2)}(-1))\\0\end{pmatrix},\end{aligned}$$

as well as

$$\begin{cases}\widetilde{\mathcal{S}}_2^{(d,1)}(p(\rho),x(\rho))=2\delta_{12}\tau_H\begin{pmatrix}x_1(0)p_2(-1)\\0\end{pmatrix},\\\widetilde{\mathcal{S}}_2^{(d,2)}(p(\rho),x(\rho))=2\delta_{12}\tau_H\begin{pmatrix}x_1(0)p_2(-1)+x_2(-1)p_1(0)\\0\end{pmatrix},\\\widetilde{\mathcal{S}}_2^{(d,3)}(p(\rho),x(\rho))=2\delta_{12}\tau_0\begin{pmatrix}x_2(-1)p_1(0)\\0\end{pmatrix}.\end{cases}$$

From (41)−(44), we have

$$(D_{z,z_x,z_{xx}}f_2^{(1,2)}(\omega,0,0))\mathcal{U}_2^{(2,d)}(\omega,0)(\rho)=\begin{pmatrix}[(D_{z,z_x,z_{xx}}\mathfrak{F}_2^d(\omega,0,0))\mathcal{U}_2^{(2,d)}(\omega,0)(\rho),\beta_{n_H}^{(1)}]\\[(D_{z,z_x,z_{xx}}\mathfrak{F}_2^d(\omega,0,0))\mathcal{U}_2^{(2,d)}(\omega,0)(\rho),\beta_{n_H}^{(2)}]\end{pmatrix},$$

and thus we obtain

$$\mathrm{Proj}_S\left((D_{z,z_x,z_{xx}}f_2^{(1,2)}(\omega,0,0))\mathcal{U}_2^{(2,d)}(\omega,0)(\rho)\right)=\mathfrak{B}(B_{24}\omega_1^2\omega_2),$$

where

$$\begin{aligned}B_{24}=\;&-\tfrac{1}{\sqrt{\iota\pi}}(\tfrac{n_H}{\iota})^2q^{\mathrm{T}}\left(\widetilde{\mathcal{S}}_2^{(d,1)}(p(\rho),\hbar_{0,11}(\rho))+\widetilde{\mathcal{S}}_2^{(d,1)}(\bar{p}(\rho),\hbar_{0,20}(\rho))\right)\\&+\tfrac{1}{\sqrt{2\iota\pi}}q^{\mathrm{T}}\textstyle\sum_{j=1,2,3}\hbar_{2n_H}^{(j)}\left(\widetilde{\mathcal{S}}_2^{(d,j)}(p(\rho),\hbar_{2n_H,11}(\rho))+\widetilde{\mathcal{S}}_2^{(d,j)}(\bar{p}(\rho),\hbar_{2n_H,20}(\rho))\right)\end{aligned}$$

with

$$\hbar_{2n_H}^{(1)}=-\frac{n_H^2}{\iota^2},\ \hbar_{2n_H}^{(2)}=2\frac{n_H^2}{\iota^2},\ \hbar_{2n_H}^{(3)}=-\frac{4n_H^2}{\iota^2}.$$

4.3. Normal form of Hopf bifurcation

Taking into account the above computations, we can obtain the normal form of Hopf bifurcation as follows:

$$\dot{\omega} = \mathfrak{D}\omega + \frac{1}{2}\begin{pmatrix} B_1\omega_1\zeta \\ \bar{B}_1\omega_2\zeta \end{pmatrix} + \frac{1}{3!}\begin{pmatrix} B_2\omega_1^2\omega_2 \\ \bar{B}_2\omega_1\omega_2^2 \end{pmatrix} + O(|\omega|\zeta^2 + |\omega|^4), \tag{51}$$

where

$$\begin{aligned} B_1 &= 2q^{\mathrm{T}}(0)\left(A_1 p(0) + (1 + i\varpi_H\sigma)A_2 p(-\hat{\sigma}) - (\tfrac{n_H}{\iota})^2 (D_1 p(0) + D_2 p(-1))\right), \\ B_2 &= B_{21} + \tfrac{3}{2}(B_{22} + B_{23} + B_{24}). \end{aligned}$$

We then utilize method [34] to rewrite normal form (51) as

$$\dot{\varrho} = K_1\varrho\zeta + K_2\varrho^3 + O(\zeta^2\varrho + |(\varrho, \zeta)|^4),$$

where

$$K_1 = \frac{1}{2}\Re(B_1),\ K_2 = \frac{1}{3!}\Re(B_2).$$

We further detect the following lemma from [45]:

Theorem 4. *The Hopf bifurcation is supercritical (subcritical) provided that $K_1K_2 < 0 (> 0)$, and the bifurcating periodic solutions are stable (unstable) if $K_2 < 0 (> 0)$.*

4.4. Calculations of Ψ_{ij}, $\mathcal{S}_2(\mathcal{P}(\rho)z_x, w)$ and $\hbar_{n,\vartheta_1\vartheta_2}(\rho)$

In order to obtain B_2, we will calculate Ψ_{ij}, $\mathcal{S}_2(\Phi(\rho)\omega_x, z)$, $\hbar_{0,20}(\rho)$, $\hbar_{0,11}(\rho)$, $\hbar_{2n_H,20}(\rho)$ and $\hbar_{2n_H,11}(\rho)$ in this subsection. We can deduce from (20) that

$$\begin{aligned} \mathfrak{F}_2(\psi, \zeta) &= \mathfrak{F}_2(\psi, 0) \\ &= f_{20000}\psi_1^2(0) + 2f_{11000}\psi_1(0)\psi_2(0) + 2f_{00110}\psi_1(-\hat{\sigma})\psi_2(-\hat{\sigma}) + f_{00020}\psi_2^2(-\hat{\sigma}) \end{aligned} \tag{52}$$

and

$$\mathfrak{F}_3(\psi, 0) = 3f_{00120}\psi_1(-\hat{\sigma})\psi_2^2(-\hat{\sigma}) + f_{00030}\psi_2^3(-\hat{\sigma}), \tag{53}$$

where

$$f_{20000} = \begin{pmatrix} -\dfrac{2r\tau_H}{K} \\ 0 \end{pmatrix}, \qquad f_{11000} = \begin{pmatrix} -b\tau_H \\ 0 \end{pmatrix}, \qquad f_{00110} = \begin{pmatrix} 0 \\ \dfrac{\tau_H\beta P_2 e^{-d\sigma}(P_2 + 2h)}{(P_2 + h)^2} \end{pmatrix},$$

$$f_{00020}=\begin{pmatrix}0\\ \dfrac{2\tau_H N_2\beta \mathrm{e}^{-d\sigma}h^2}{(P_2+h)^3}\end{pmatrix},\qquad f_{00120}=\begin{pmatrix}0\\ \dfrac{2\tau_H \beta \mathrm{e}^{-d\sigma}h^2}{(P_2+h)^3}\end{pmatrix},$$
$$f_{00030}=\begin{pmatrix}0\\ \dfrac{-6\tau_H \beta \mathrm{e}^{-d\sigma}N_2h^2}{(P_2+h)^4}\end{pmatrix}.$$

Letting

$$\begin{aligned}\psi(\rho)&=\mathcal{P}(\rho)\omega_x=p(\rho)\omega_1(t)b_{n_H}(x)+\overline{p}(\rho)\omega_2(t)b_{n_H}(x)\\&=\begin{pmatrix}p_1(\rho)\omega_1(t)b_{n_H}(x)+\overline{p}_1(\rho)\omega_2(t)b_{n_H}(x)\\ p_2(\rho)\omega_1(t)b_{n_H}(x)+\overline{p}_2(\rho)\omega_2(t)b_{n_H}(x)\end{pmatrix}\\&=\begin{pmatrix}\psi_1(\rho)\\ \psi_2(\rho)\end{pmatrix},\end{aligned}\tag{54}$$

we have

$$\mathfrak{F}_2(\mathcal{P}(\rho)\omega_x,0)=\textstyle\sum_{\vartheta_1+\vartheta_2=2} b_n^{\vartheta_1+\vartheta_2=2}(x)\Psi_{\vartheta_1\vartheta_2}\omega_1^{\vartheta_1}\omega_2^{\vartheta_2},\tag{55}$$

then in conjunction with (52), (54) and (55), we obtain

$$\begin{aligned}\Psi_{20}=&f_{20000}p_1^2(0)+2f_{11000}p_1(0)p_2(0)+2f_{00110}p_1(-\hat{\sigma})p_2(-\hat{\sigma})+f_{00020}p_2^2(-\hat{\sigma}),\\ \Psi_{11}=&2\Big(f_{00020}p_2(-\hat{\sigma})\overline{p}_2(-\hat{\sigma})+f_{00110}\overline{p}_1(-\hat{\sigma})p_2(-\hat{\sigma})+f_{00110}p_1(-\hat{\sigma})\overline{p}_2(-\hat{\sigma})\\&+f_{11000}\overline{p}_1(0)p_2(0)+f_{11000}p_1(0)\overline{p}_2(0)+f_{20000}p_1(0)\overline{p}_1(0)\Big),\\ \Psi_{02}=&f_{00020}\overline{p}_2^2(-\hat{\sigma})+2f_{00110}\overline{p}_1(-\hat{\sigma})\overline{p}_2(-\hat{\sigma})+2f_{11000}\overline{p}_1(0)\overline{p}_2(0)+f_{20000}\overline{p}_1^2(0).\end{aligned}$$

Furthermore, it follows from (45), (53) and (54) that

$$\begin{aligned}\Psi_{30}&=p_2^2(-\hat{\sigma})\Big(f_{00030}p_2(-\hat{\sigma})+3f_{00120}p_1(-\hat{\sigma})\Big),\\ \Psi_{21}&=3p_2(-\hat{\sigma})\Big(f_{00030}p_2(-\hat{\sigma})\overline{p}_2(-\hat{\sigma})+f_{00120}p_2(-\hat{\sigma})\overline{p}_1(-\hat{\sigma})+2f_{00120}p_1(-\hat{\sigma})\overline{p}_2(-\hat{\sigma})\Big),\\ \Psi_{12}&=3\overline{p}_2(-\hat{\sigma})\Big(f_{00030}p_2(-\hat{\sigma})\overline{p}_2(-\hat{\sigma})+2f_{00120}p_2(-\hat{\sigma})\overline{p}_1(-\hat{\sigma})+2f_{00120}p_1(-\hat{\sigma})\overline{p}_2(-\hat{\sigma})\Big),\\ \Psi_{03}&=\overline{p}_2^2(-\hat{\sigma})\Big(f_{00030}\overline{p}_2(-\hat{\sigma})+3f_{00120}\overline{p}_1(-\hat{\sigma})\Big).\end{aligned}$$

Similarly, we have

$$\begin{aligned}\mathfrak{F}_2(\mathcal{P}(\rho)\omega_x+z,\zeta)=&\mathfrak{F}_2(\mathcal{P}(\rho)\omega_x+z,0)\\=&\sum_{\vartheta_1+\vartheta_2=2} b_n^{\vartheta_1+\vartheta_2=2}(x)\Psi_{\vartheta_1\vartheta_2}\omega_1^{\vartheta_1}\omega_2^{\vartheta_2}+\mathcal{S}_2(\mathcal{P}(\rho)\omega_x,z)+O(|z|^2),\end{aligned}$$

where

$$\begin{aligned}\mathcal{S}_2(\mathcal{P}(\rho)\omega_x, z) =& 2\Big(f_{00110}p_2(-\hat{\sigma})z_1(-\hat{\sigma}) + \big(f_{00020}p_2(-\hat{\sigma}) + f_{00110}p_1(-\hat{\sigma})\big)z_2(-\hat{\sigma})\\ &+ \big(f_{11000}p_2(0) + f_{20000}p_1(0)\big)z_1(0) + f_{11000}p_1(0)z_2(0)\Big)b_n(x)\omega_1\\ &+ 2\Big(f_{00110}\overline{p}_2(-\hat{\sigma})z_1(-\hat{\sigma}) + \big(f_{00020}\overline{p}_2(-\hat{\sigma}) + f_{00110}\overline{p}_1(-\hat{\sigma})\big)z_2(-\hat{\sigma})\\ &+ \big(f_{11000}\overline{p}_2(0) + f_{20000}\overline{p}_1(0)\big)z_1(0) + f_{11000}\overline{p}_1(0)z_2(0)\Big)b_n(x)\omega_2.\end{aligned}$$

Next, we will calculate $\hbar_{0,20}(\rho)$, $\hbar_{0,11}(\rho)$, $\hbar_{2n_H,20}(\rho)$ and $\hbar_{2n_H,11}(\rho)$. It follows from [43, 46] that

$$M_2^2(\hbar_n(\rho,\omega)b_n(x)) = D_\omega(\hbar_n(\rho,\omega)b_n(x))\mathfrak{D}\omega - \mathcal{A}_{\mathcal{Q}^1}(\hbar_n(\rho,\omega)b_n(x)),$$

which results in

$$\begin{aligned}\begin{pmatrix}[M_2^2(\hbar_n(\rho,\omega)b_n(x)), \beta_n^{(1)}]\\ [M_2^2(\hbar_n(\rho,\omega)b_n(x)), \beta_n^{(2)}]\end{pmatrix} =& \quad 2i\varpi_H\tau_H(\hbar_{n,20}(\rho)\omega_1^2 - \hbar_{n,02}(\rho)\omega_2^2)\\ &-\Big(\dot{\hbar}_n(\rho,\omega) + Y_0(\rho)(\mathfrak{L}_0(\hbar_n(\rho,\omega)) - \dot{\hbar}_n(0,\omega))\Big),\end{aligned}$$

where

$$\mathfrak{L}_0(\hbar_n(\rho,\omega)) = \tau_H\Big(A_1\hbar_n(0,\omega) + A_2\hbar_n(-\hat{\sigma},\omega) - (\frac{n}{\iota})^2\Big(D_1\hbar_n(0,\omega) + D_2\hbar_n(-1,\omega)\Big)\Big).$$

By combining with (25) and (26), we obtain

$$\begin{aligned}f_2^2(\omega,0,0) &= Y_0(\rho)\tilde{\mathfrak{F}}_2(\mathcal{P}(\rho)\omega_x,0) - \pi(Y_0(\rho)\tilde{\mathfrak{F}}_2(\mathcal{P}(\rho)\omega_x,0))\\ &= Y_0(\rho)\tilde{\mathfrak{F}}_2(\mathcal{P}(\rho)\omega_x,0) - \mathcal{P}(\rho)\mathcal{Q}(0)\begin{pmatrix}[\tilde{\mathfrak{F}}_2(\mathcal{P}(\rho)\omega_x,0), \beta_{n_H}^{(1)}]\\ [\tilde{\mathfrak{F}}_2(\mathcal{P}(\rho)\omega_x,0), \beta_{n_H}^{(2)}]\end{pmatrix}b_n(x).\end{aligned}$$

It then follows from (46), (47) and (48) that

$$\begin{pmatrix}[f_2^2(\omega,0,0), \beta_n^{(1)}]\\ [f_2^2(\omega,0,0), \beta_n^{(2)}]\end{pmatrix} = \begin{cases}\frac{1}{\sqrt{\iota\pi}}Y_0(\rho)\Big(\Psi_{20}\omega_1^2 + \Psi_{02}\omega_2^2 + \Psi_{11}\omega_1\omega_2\Big), & n=0,\\ \frac{1}{\sqrt{2\iota\pi}}Y_0(\rho)\Big(\tilde{\Psi}_{20}\omega_1^2 + \tilde{\Psi}_{02}\omega_2^2 + \tilde{\Psi}_{11}\omega_1\omega_2\Big), & n=2n_H,\end{cases}$$

where $\tilde{\Psi}_{i_1i_2}$ is given by

$$\begin{cases}\tilde{\Psi}_{i_1i_2} = \Psi_{i_1i_2} - 2(\frac{n_H}{\iota})^2\Psi^d_{i_1i_2},\\ i_1,i_2 = 0,1,2,\ i_1+i_2=2,\end{cases} \tag{56}$$

where $\Psi^d_{i_1 i_2}$ is given by (49). Thereupon, we match the coefficients of ω_1^2 and $\omega_1\omega_2$ to get

$$n=0,\begin{cases}\omega_1^2:\begin{cases}\dot{\hbar}_{0,20}(\rho)-2i\varpi_H\tau_H\hbar_{0,20}(\rho)=(0,0)^{\mathrm{T}},\\ \dot{\hbar}_{0,20}(0)-\mathcal{L}_0(\hbar_{0,20}(\rho))=\frac{1}{\sqrt{\iota\pi}}\Psi_{20},\end{cases}\\ \omega_1\omega_2:\begin{cases}\dot{\hbar}_{0,11}(\rho)=(0,0)^{\mathrm{T}},\\ \dot{\hbar}_{0,11}(0)-\mathcal{L}_0(\hbar_{0,11}(\rho))=\frac{1}{\sqrt{\iota\pi}}\Psi_{11},\end{cases}\end{cases}\tag{57}$$

and

$$n=2n_H,\begin{cases}\omega_1^2:\begin{cases}\dot{\hbar}_{2n_H,20}(\rho)-2i\varpi_H\tau_H\hbar_{2n_H,20}(\rho)=(0,0)^{\mathrm{T}},\\ \dot{\hbar}_{2n_H,20}(0)-\mathfrak{L}_0(\hbar_{2n_H,20}(\rho))=\frac{1}{\sqrt{2\iota\pi}}\tilde{\Psi}_{20},\end{cases}\\ \omega_1\omega_2:\begin{cases}\dot{\hbar}_{2n_H,20}(\rho)=(0,0)^{\mathrm{T}},\\ \dot{\hbar}_{2n_H,11}(0)-\mathfrak{L}_0(\hbar_{2n_H,11}(\rho))=\frac{1}{\sqrt{2\iota\pi}}\tilde{\Psi}_{11}.\end{cases}\end{cases}\tag{58}$$

We solve from (57) that $\hbar_{0,20}(\rho)=\mathrm{e}^{2i\varpi_H\tau_H\rho}\hbar_{0,20}(0)$ and hence $\hbar_{0,20}(-\hat{\sigma})=\mathrm{e}^{-2i\varpi_H\sigma}\hbar_{0,20}(0)$. We then have

$$(2i\varpi_H\tau_H E_2-\tau_H A_1-\tau_H A_2\mathrm{e}^{-2i\varpi_H\sigma})\hbar_{0,20}(0)=\frac{1}{\sqrt{\iota\pi}}\Psi_{20},$$

and hence

$$\hbar_{0,20}(\rho)=\mathrm{e}^{2i\varpi_H\tau_H\rho}\left(2i\varpi_H\tau_H E_2-\tau_H A_1-\tau_H A_2\mathrm{e}^{-2i\varpi_H\sigma}\right)^{-1}\frac{1}{\sqrt{\iota\pi}}\Psi_{20}.$$

Similarly, we can obtain

$$\hbar_{0,11}(\rho)=(-\tau_H A_1-\tau_H A_2)^{-1}\frac{1}{\sqrt{\iota\pi}}\Psi_{11}.$$

Also, we can solve from (58) that $\hbar_{2n_H,20}(\rho)=\mathrm{e}^{2i\varpi_H\tau_H\rho}\hbar_{2n_H,20}(0)$ and hence $\hbar_{2n_H,20}(-1)=\mathrm{e}^{-2i\varpi_H\tau_H}\hbar_{2n_H,20}(0)$ and $\hbar_{2n_H,20}(-\hat{\sigma})=\mathrm{e}^{-2i\varpi_H\sigma}\hbar_{2n_H,20}(0)$. Noticing that

$$\begin{aligned}\mathfrak{L}_0(\hbar_{2n_H,20}(\rho))=&-\tau_H\frac{4n_H^2}{\iota^2}(D_1\hbar_{2n_H,20}(0)+D_2\hbar_{2n_H,20}(-1))\\&+\tau_H A_1\hbar_{2n_H,20}(0)+\tau_H A_2\hbar_{2n_H,20}(-\hat{\sigma}),\end{aligned}$$

we obtain

$$\begin{aligned}&\left(2i\varpi_H\tau_H E_2+\tau_H\frac{4n_H^2}{\iota^2}D_1+\tau_H\frac{4n_H^2}{\iota^2}D_2\mathrm{e}^{-2i\varpi_H\tau_H}-\tau_H A_1-\tau_H A_2\mathrm{e}^{-2i\varpi_0\sigma}\right)\hbar_{2n_H,20}(0)\\&=\frac{1}{\sqrt{2\iota\pi}}\tilde{\Psi}_{20},\end{aligned}$$

and hence

$$\hbar_{2n_H,20}(\rho) = \mathrm{e}^{2i\varpi_H\tau_H\rho}\Big(2i\varpi_H E_2 + \frac{4n_H^2}{\iota^2}D_1 + \frac{4n_H^2}{\iota^2}D_2\mathrm{e}^{-2i\varpi_H\tau_H} - A_1 - A_2\mathrm{e}^{-2i\varpi_H\sigma}\Big)^{-1}\frac{\tilde{\Psi}_{20}}{\sqrt{2\iota\pi}\,\tau_H},$$

where $\tilde{\Psi}_{20}$ is given by (56). Similarly, we have

$$\hbar_{2n_H,11}(\rho) = \Big(\tau_H\frac{4n_H^4}{\iota^2}D_1 + \tau_H\frac{4n_H^4}{\iota^2}D_2 - \tau_H A_1 - \tau_H A_2\Big)^{-1}\frac{1}{\sqrt{2\iota\pi}}\tilde{\Psi}_{11}.$$

5. Discussion

Understanding the distribution of species in space according to biotic processes and environmental elements has been rated among the five top ecological research fronts [47]. However the effects of memory-dependent movement along with other biological processes on the spatial patterns of species have not been studied in depth. In this regard, we propose a class of spatial predator-prey model with Allee effect, memory delay and (maturation) delay-dependent coefficients. We first study the model without delay and found that the biomass of predators tends to extinction as the intensity of Allee effect is large enough, see Remark 1. Under the prerequisite that Allee effect is not too strong so that hypothesis (H1) is satisfied, we further explore the joint effects of memory delay and maturation delay on the coexisting constant steady state $E_2(\sigma)$. By appealing to the method set forth in [35], we obtain the stability crossing curves on the (σ,τ) plane such that the characteristic equation (8) has at least one pair of purely imaginary roots when (σ,τ) is on the crossing curves, and based on which we discern the stable regions. To further determine the direction of Hopf bifurcation and the stability of the bifurcating periodic solutions, we calculate the coefficients for normal form of Hopf bifurcation induced by memory delay. Our algorithm presents a refinement of that given in [34].

To confirm the theoretical results obtained, we present a numerical illustration here. We fix the parameters $r=2,\ K=4,\ b=1.2,\ \beta=0.96,\ d=0.2,\ h=0.4,\ \mu=0.5,\ \delta_{11}=0.1,\ \delta_{12}=0.4,\ \delta_{22}=0.1,\ \iota=2\pi$. According to Theorem 2, we can first determine that the stable intervals of $E_2(\sigma)$ for maturation delay σ is $[0,0.5566)\cup(2.2348,5.4715)$. We then display the joint effects of maturation delay and memory delay on the dynamics of model (2). According to the method developed in Sect. 3, we can obtain the crossing curves $\mathcal{T}^n$ for $n\le 7$ as displayed in Fig. 2. The linear stable region in Fig. 2 includes two parts: the bottom left one and right one. The right boundary of the bottom left region is consisted of the lower left sections of all crossing curves $\mathcal{T}^n$, and the left boundary of the bottom right one is consisted of the lower right sections of all crossing curves $\mathcal{T}^n$. The stability of $E_2(\sigma)$ changes when (σ,τ) passes through these boundaries. In this case, stable spatially inhomogeneous periodic solutions with mode-n spatial pattern are prone to occur which is strikingly different from previous models without memory delay [22]. For example, for fixed $\sigma=3.1$, we can calculate $n_H=4,\ \varpi_H^4\approx 0.4051,\ \tau_H^4\approx 2.3929,\ K_1\approx 0.0138>0,\ K_2\approx -0.0503<0$ according to the formulae given in Sect. 4. This indicates that a mode-4 spatially inhomogeneous Hopf bifurcation occurs at $\tau=\tau_H^4$. By Theorem 4 we know that it is supercritical and the bifurcating spatially inhomogeneous periodic solutions with mode-4 spatial pattern are stable. We finally pick points P_1-P_6 in Fig. 2 as the values of (σ,τ) for simulations which are displayed in Fig. 3. These

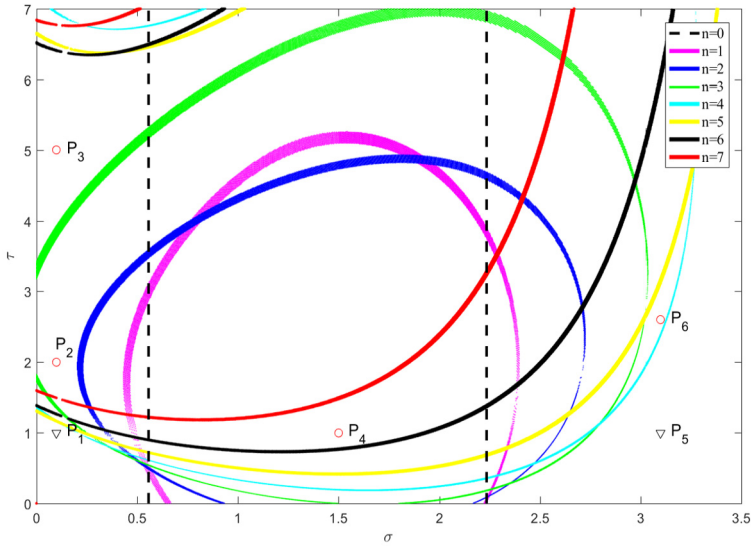

Fig. 2. Crossing curves in the (σ, τ) plane with $n \leq 7$. The points $P_1(0.1, 1)$, $P_2(0.1, 2)$, $P_3(0.1, 5)$, $P_4(1.5, 1)$, $P_5(3.1, 1)$ and $P_6(3.1, 2.6)$ are chosen for further simulations.

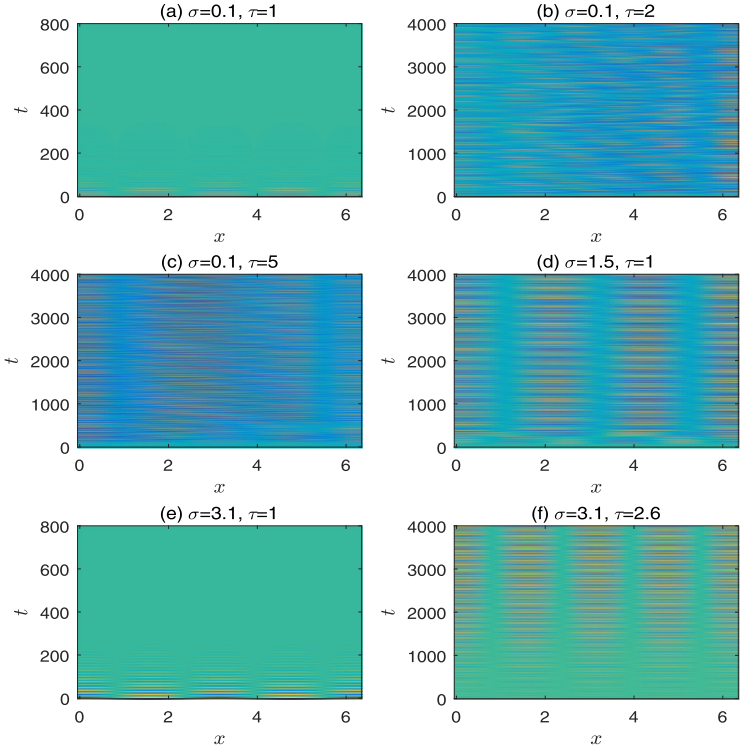

Fig. 3. The spatial-temporal diagrams of $P(x,t)$ for model (2) with $N(x,t) = N_2(\sigma) + 0.01\cos(2x)$ and $P(x,t) = P_2(\sigma) + 0.01\cos(2x)$, $t \in [-\max\{\tau, \sigma\}, 0]$. The values of (σ, τ) for Figs. (a)-(f) are respectively the values of the point P_1 to P_6.

simulations illustrate that stability switches occur as (σ, τ) moves from P_1 to P_4 to P_5 (see the three subgraphs on the left panel from above down), and a stable spatially inhomogeneous periodic solution with mode-4 spatial pattern appears as memory delay τ passes through the Hopf bifurcation point τ_H^4 for fixed $\sigma = 3.1$ (see subgraphs (e) and (f)).

Our method developed in this paper can be applied to the following model with spatial memory in predators:

$$\begin{cases} \frac{\partial N}{\partial t} = \delta_{11} N_{xx} + rN\Big(1 - \frac{N}{K}\Big) - bNP, \ 0 < x < \iota\pi, \ t > 0, \\ \frac{\partial P}{\partial t} = \delta_{22} P_{xx} - \delta_{21}\big(PN_x(x, t-\tau)\big)_x + \frac{\beta N_\sigma P_\sigma^2}{h + P_\sigma} \mathrm{e}^{-d\sigma} - \mu P, \ 0 < x < \iota\pi, \ t > 0, \\ N_x(0,t) = N_x(\iota\pi, t) = P_x(0,t) = P_x(\iota\pi, t) = 0, \ t \geq 0, \end{cases} \tag{59}$$

where τ is the average memory period of predators, and δ_{21} is the memory-dependent diffusion coefficient with the sign "$-$" describing predators having the tendency to move to high-density positions of the prey. Model (59) can characterize some highly developed animals with prior knowledge of the prey distribution [48]. For example, whales move according to the accumulation of information in space since they possess a memory of over 10 years [49]. Analyzing similarly as in Sect. 3 for model (2), we can easily obtain the associated characteristic equation of model (59) as follows:

$$\mathfrak{g}_0^n(\lambda, \sigma) + \mathfrak{g}_1^n(\lambda, \sigma)\mathrm{e}^{-\lambda\sigma} - \delta_{21} P_i(\sigma)\alpha_{12}(\sigma)\Big(\frac{n}{\iota}\Big)^2 \mathrm{e}^{-\lambda\tau} = 0.$$

We can also obtain the functions $\mathcal{S}_\kappa(\sigma)$, stability crossing curves $\mathcal{T}^n$ as well as normal form of Hopf bifurcation with some small modifications.

We compare the dynamics between models (59) and (2) via another numerical example. We choose $\delta_{21} = 0.4$ and other parameters take the same values as in the previous numerical example. Similarly, we can calculate that the stable intervals of $E_2(\sigma)$ for maturation delay σ is $[0, 0.5566) \cup (2.2348, 5.4715)$. We can further plot crossing curves $\mathcal{T}^n, n = 1, 2, \cdots 7$ in the region of (σ, τ), $[0, 5.3] \times [0, 7]$, as shown in Fig. 4. Compared with Fig. 2, we can observe that there exist spiral-like curves along σ axis. We also observe that all stability crossing curves do not intersect with the σ-axis. This indicates that the bifurcation periodic solutions of model (59) without memory delay are spatially homogeneous. Similarly, for $\sigma = 2.5$, we can calculate $n_H = 7$, $\varpi_H^7 \approx 2.4976$, $\tau_H^7 \approx 0.4489$, $K_1 \approx 0.4285 > 0$ and $K_2 \approx -0.0079 < 0$ which indicates that a stable spatially inhomogeneous periodic solution with mode-7 spatial pattern appears as τ passes τ_H^7 in the increasing direction with spatially inhomogeneous initial functions as shown in Fig. 5. We also observe that the solution of model (59) with spatially homogeneous initial functions tends to the constant steady state $E_2(2.5)$ as τ passes through τ_H^7 in the increasing direction as shown in Fig. 6. These reflect that the initial values can significantly affect the long-time behavior of memory-based diffusion models.

To summarize, the model and methodology developed in this paper provide a new avenue to study spatiotemporal models with spatial memory and to understand the distribution of species in space and time. There are many interesting problems deserving further investigation. For example, spatial memory may exist in both predators and the prey, how to deal with this kind of models and obtain their associated stability crossing curves is a challenging problem. In addition, we observe from Figs. 2 and 4 that the crossing curves can intersect at some points. These points

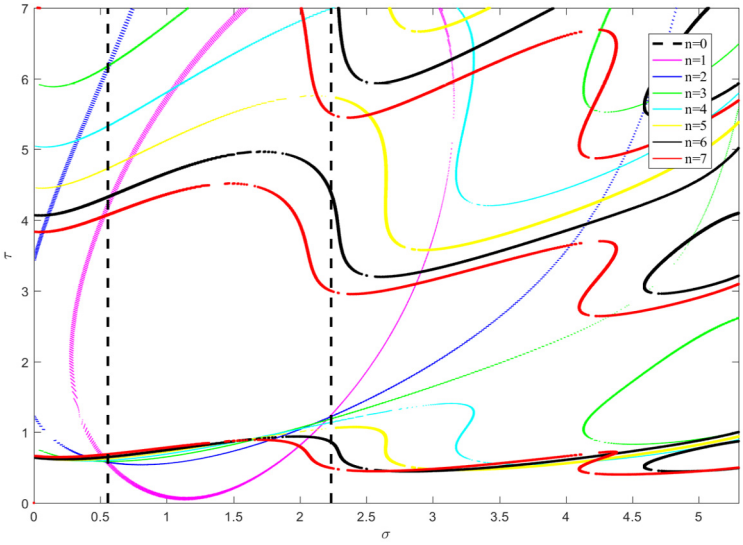

Fig. 4. Crossing curves in the (σ, τ) plane with $n \leq 7$ for model (59).

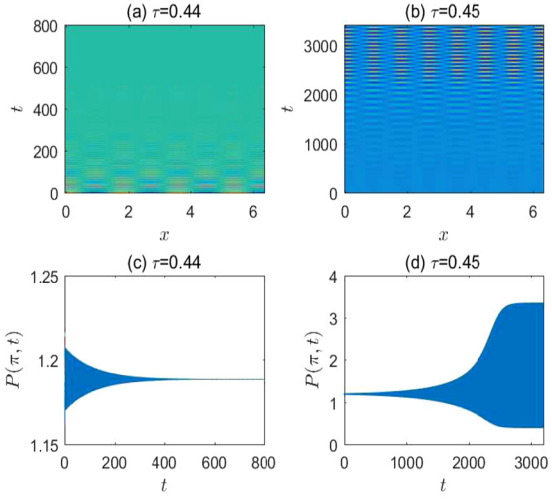

Fig. 5. The spatial-temporal diagrams and time series at location $x = \pi$ of P for model (59) with $N(x,t) = N_2(2.5) + 0.01\cos(\frac{7x}{2})$ and $P(x,t) = P_2(2.5) + 0.01\cos(\frac{7x}{2})$, $t \in [-\max\{\tau, \sigma\}, 0]$.

are dubbed double Hopf bifurcation points. Generally, the model can exhibit complicated dynamics such as quasi-periodic solutions and even chaos when the parameters of model are taken around such points [50]. Therefore, how to obtain the normal form of double Hopf bifurcation induced by memory and maturation delays deserves further consideration. Finally, the distributions of resources are usually not homogeneous in space, how will the distribution of the species change when parameters of model are dependent on location x? We leave all these for our future consideration.

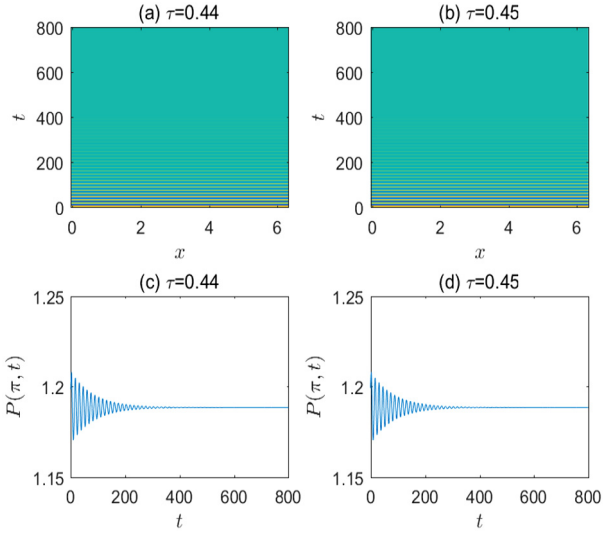

Fig. 6. The spatial-temporal diagrams and time series at location $x = \pi$ of P for model (59) with $N(x,t) = N_2(2.5) + 0.01$ and $P(x,t) = P_2(2.5) + 0.01,\ t \in [-\max\{\tau,\sigma\}, 0]$.

Declaration of competing interest

The authors declare that they have no known competing financial interests or personal relationships that could have appeared to influence the work reported in this paper.

CRediT authorship contribution statement

All authors contributed equally to this work.

Data availability

No data was used for the research described in the article.

Acknowledgments

The authors would like to thank both the editor and the reviewer for their valuable comments and suggestions, which have greatly improved the quality and presentation of our paper. The first two authors are partially supported by the National Natural Science Foundation of China (grant number: 12071293). The fourth author is partially supported by the Natural Sciences and Engineering Research Council of Canada (Discovery Grant RGPIN-2020-03911 and Accelerator Grant RGPAS-2020-00090).

References

[1] A.J. Lotka, Undamped oscillations derived from the law of mass action, J. Am. Chem. Soc. 42 (8) (1920) 1595–1599, https://doi.org/10.1021/ja01453a010.

[2] V. Volterra, Variazioni e fluttuazioni del numero d'individui in specie animali conviventi, Mem. Accad. Lincei 15 (1–2) (1926) 31–71, https://doi.org/10.1002/iroh.19260150103.

[3] W.C. Allee, Animal aggregations, Q. Rev. Biol. 2 (3) (1927) 367–398, https://doi.org/10.1086/394281.
[4] B. Dennis, Allee effects: population growth, critical density, and the chance of extinction, Nat. Resour. Model. 3 (4) (1989) 481–538, https://doi.org/10.1111/j.1939-7445.1989.tb00119.x.
[5] M. Fowler, G. Ruxton, Population dynamic consequences of Allee effects, J. Theor. Biol. 215 (1) (2002) 39–46, https://doi.org/10.1006/jtbi.2001.2486.
[6] L. Berec, E. Angulo, F. Courchamp, Multiple Allee effects and population management, Trends Ecol. Evol. 22 (4) (2007) 185–191, https://doi.org/10.1016/j.tree.2006.12.002.
[7] M.A. Lewis, P. Kareiva, Allee dynamics and the spread of invading organisms, Theor. Popul. Biol. 43 (2) (1993) 141–158, https://doi.org/10.1006/jtbi.2001.2486.
[8] D.S. Boukal, M.W. Sabelis, L. Berec, How predator functional responses and Allee effects in prey affect the paradox of enrichment and population collapses, Theor. Popul. Biol. 72 (1) (2007) 136–147, https://doi.org/10.1016/j.tpb.2006.12.003.
[9] X.X. Guo, Z.M. Guo, A Markov-switching predator–prey model with Allee effect for preys, Int. J. Biomath. 13 (03) (2020) 2050018, https://doi.org/10.1142/S1793524520500187.
[10] D.Y. Wu, H.Y. Zhao, Spatiotemporal dynamics of a diffusive predator–prey system with Allee effect and threshold hunting, J. Nonlinear Sci. 30 (3) (2020) 1015–1054, https://doi.org/10.1007/s00332-019-09600-0.
[11] D. Sen, S. Ghorai, M. Banerjee, A. Morozov, Bifurcation analysis of the predator–prey model with the Allee effect in the predator, J. Math. Biol. 84 (1) (2022) 1–27, https://doi.org/10.1007/s00285-021-01707-x.
[12] S. Rana, S. Bhattacharya, S. Samanta, Complex dynamics of a three-species food chain model with fear and Allee effect, Int. J. Bifurc. Chaos 32 (6) (2022) 2250084, https://doi.org/10.1142/S0218127422500845.
[13] S. Rana, A.R. Bhowmick, T. Sardar, Invasive dynamics for a predator–prey system with Allee effect in both populations and a special emphasis on predator mortality, Chaos 31 (3) (2021) 033150, https://doi.org/10.1063/5.0035566.
[14] Y. Kuang, J.W.-H. So, Analysis of a delayed two-stage population model with space-limited recruitment, SIAM J. Appl. Math. 55 (6) (1995) 1675–1696, https://doi.org/10.1137/S0036139993252839.
[15] S.A. Gourley, Y. Kuang, A stage structured predator-prey model and its dependence on maturation delay and death rate, J. Math. Biol. 49 (2) (2004) 188–200, https://doi.org/10.1007/s00285-004-0278-2.
[16] P. Wu, H.Y. Zhao, Dynamical analysis of a nonlocal delayed and diffusive HIV latent infection model with spatial heterogeneity, J. Franklin Inst. 358 (10) (2021) 5552–5587, https://doi.org/10.1016/j.jfranklin.2021.05.014.
[17] E. Beretta, Y. Kuang, Geometric stability switch criteria in delay differential systems with delay dependent parameters, SIAM J. Math. Anal. 33 (5) (2002) 1144–1165, https://doi.org/10.1137/S0036141000376086.
[18] C. Jin, K.Q. Gu, S.-I. Niculescu, I. Boussaada, Stability analysis of systems with delay-dependent coefficients: an overview, IEEE Access 6 (2018) 27392–27407, https://doi.org/10.1109/ACCESS.2018.2828871.
[19] X.F. Xu, J.J. Wei, Bifurcation analysis of a spruce budworm model with diffusion and physiological structures, J. Differ. Equ. 262 (10) (2017) 5206–5230, https://doi.org/10.1016/j.jde.2017.01.023.
[20] Y.F. Du, B. Niu, Y.X. Guo, J.J. Wei, Double Hopf bifurcation in delayed reaction–diffusion systems, J. Dyn. Differ. Equ. 32 (1) (2020) 313–358, https://doi.org/10.1007/s10884-018-9725-4.
[21] M. Banerjee, S. Petrovskii, Self-organised spatial patterns and chaos in a ratio-dependent predator–prey system, Theor. Ecol. 4 (1) (2011) 37–53, https://doi.org/10.1007/s12080-010-0073-1.
[22] Z.C. Jiang, M.W. Nie, Persistence and bifurcation analysis of a plankton ecosystem with cross-diffusion and double delays, Int. J. Bifurc. Chaos 32 (02) (2022) 2250017, https://doi.org/10.1142/S0218127422500171.
[23] R. Nathan, W.M. Getz, E. Revilla, M. Holyoak, R. Kadmon, D. Saltz, P.E. Smouse, A movement ecology paradigm for unifying organismal movement research, Proc. Natl. Acad. Sci. USA 105 (49) (2008) 19052–19059, https://doi.org/10.1073/pnas.0800375105.
[24] J. Liu, Qualitative analysis of a diffusive predator–prey model with Allee and fear effects, Int. J. Biomath. 14 (06) (2021) 2150037, https://doi.org/10.1142/S1793524521500376.
[25] H. Wang, Y. Salmaniw, Open problems in PDE models for cognitive animal movement via nonlocal perception and mental mapping, arXiv preprint, arXiv:2201.09150.
[26] J. Berger, Pregnancy incentives, predation constraints and habitat shifts: experimental and field evidence for wild bighorn sheep, Anim. Behav. 41 (1) (1991) 61–77, https://doi.org/10.1016/S0003-3472(05)80503-2.
[27] W.F. Fagan, M.A. Lewis, M. Auger-Méthé, T. Avgar, S. Benhamou, G. Breed, L. LaDage, U.E. Schlägel, W.-w. Tang, Y.P. Papastamatiou, et al., Spatial memory and animal movement, Ecol. Lett. 16 (10) (2013) 1316–1329, https://doi.org/10.1111/ele.12165.
[28] B. Gehr, N.C. Bonnot, M. Heurich, F. Cagnacci, S. Ciuti, A.M. Hewison, J.-M. Gaillard, N. Ranc, J. Premier, K. Vogt, et al., Stay home, stay safe—site familiarity reduces predation risk in a large herbivore in two contrasting study sites, J. Anim. Ecol. 89 (6) (2020) 1329–1339, https://doi.org/10.1111/1365-2656.13202.

[29] C.H. Wang, S.L. Yuan, H. Wang, Spatiotemporal patterns of a diffusive prey-predator model with spatial memory and pregnancy period in an intimidatory environment, J. Math. Biol. 84 (3) (2022) 1–36, https://doi.org/10.1007/s00285-022-01716-4.
[30] A. Lafontaine, P. Drapeau, D. Fortin, M.-H. St-Laurent, Many places called home: the adaptive value of seasonal adjustments in range fidelity, J. Anim. Ecol. 86 (3) (2017) 624–633, https://doi.org/10.1111/1365-2656.12645.
[31] A. Falcón-Cortés, D. Boyer, E.H. Merrill, J.L. Frair, J.M. Morales, Hierarchical, memory-based movement models for translocated Elk (Cervus canadensis), Front. Ecol. Evol. (2021) 497, https://doi.org/10.3389/fevo.2021.702925.
[32] J.P. Shi, C.C. Wang, H. Wang, X.P. Yan, Diffusive spatial movement with memory, J. Dyn. Differ. Equ. 32 (2) (2020) 979–1002, https://doi.org/10.1007/s10884-019-09757-y.
[33] Y.L. Song, J.P. Shi, H. Wang, Spatiotemporal dynamics of a diffusive consumer-resource model with explicit spatial memory, Stud. Appl. Math. 148 (1) (2022) 373–395, https://doi.org/10.1111/sapm.12443.
[34] Y.L. Song, Y.H. Peng, T.H. Zhang, The spatially inhomogeneous Hopf bifurcation induced by memory delay in a memory-based diffusion system, J. Differ. Equ. 300 (2021) 597–624, https://doi.org/10.1016/j.jde.2021.08.010.
[35] Q. An, E. Beretta, Y. Kuang, C.C. Wang, H. Wang, Geometric stability switch criteria in delay differential equations with two delays and delay dependent parameters, J. Differ. Equ. 266 (11) (2019) 7073–7100, https://doi.org/10.1016/j.jde.2018.11.025.
[36] Y.H. Lv, The spatially homogeneous Hopf bifurcation induced jointly by memory and general delays in a diffusive system, Chaos Solitons Fractals 156 (2022) 111826, https://doi.org/10.1016/j.chaos.2022.111826.
[37] M. Liu, H.B. Wang, W.H. Jiang, Bifurcations and pattern formation in a predator-prey model with memory-based diffusion, J. Differ. Equ. 350 (2023) 1–40, https://doi.org/10.1016/j.jde.2022.12.010.
[38] S.L. Robertson, S.M. Henson, T. Robertson, J. Cushing, A matter of maturity: to delay or not to delay? Continuous-time compartmental models of structured populations in the literature 2000–2016, Nat. Resour. Model. 31 (1) (2018) e12160, https://doi.org/10.1111/nrm.12160.
[39] W.X. Xu, H.Y. Shu, Z. Tang, W. Hao, Complex dynamics in a general diffusive predator-prey model with predator maturation delay, J. Dyn. Differ. Equ. (2022), https://doi.org/10.1007/s10884-022-10176-9.
[40] L. Perko, Differential Equations and Dynamical Systems, vol. 7, Springer Science & Business Media, 2001.
[41] K.Q. Gu, S.-I. Niculescu, J. Chen, On stability crossing curves for general systems with two delays, J. Math. Anal. Appl. 311 (1) (2005) 231–253, https://doi.org/10.1016/j.jmaa.2005.02.034.
[42] X.H. Lin, H. Wang, Stability analysis of delay differential equations with two discrete delays, Can. Appl. Math. Q. 20 (4) (2012) 519–533.
[43] T. Faria, Normal forms and Hopf bifurcation for partial differential equations with delays, Trans. Am. Math. Soc. 352 (5) (2000) 2217–2238, https://doi.org/10.1090/S0002-9947-00-02280-7.
[44] S.J. Guo, Theory and applications of equivariant normal forms and Hopf bifurcation for semilinear FDEs in Banach spaces, J. Differ. Equ. 317 (2022) 387–421, https://doi.org/10.1016/j.jde.2022.02.016.
[45] S.-N. Chow, J.K. Hale, Methods of Bifurcation Theory, Springer-Verlag, New York, 1982.
[46] J. Wu, Theory and Applications of Partial Functional Differential Equations, vol. 119, Springer Science & Business Media, 1996.
[47] I.W. Renner, D.I. Warton, Equivalence of MAXENT and Poisson point process models for species distribution modeling in ecology, Biometrics 69 (1) (2013) 274–281, https://doi.org/10.1111/j.1541-0420.2012.01824.x.
[48] J.A. Merkle, D. Fortin, J.M. Morales, A memory-based foraging tactic reveals an adaptive mechanism for restricted space use, Ecol. Lett. 17 (8) (2014) 924–931, https://doi.org/10.1111/ele.12294.
[49] B. Abrahms, E.L. Hazen, E.O. Aikens, M.S. Savoca, J.A. Goldbogen, S.J. Bograd, M.G. Jacox, L.M. Irvine, D.M. Palacios, B.R. Mate, Memory and resource tracking drive blue whale migrations, Proc. Natl. Acad. Sci. USA 116 (12) (2019) 5582–5587, https://doi.org/10.1073/pnas.1819031116.
[50] D.X. Geng, H.B. Wang, Normal form formulations of double- Hopf bifurcation for partial functional differential equations with nonlocal effect, J. Differ. Equ. 309 (2022) 741–785, https://doi.org/10.1016/j.jde.2021.11.046.